Final Report of K-125174 project entitled "Physiological and pathophysiological functions of lysophosphatidic acid receptors in the cardiovascular system."

Effects of lysophosphatidic acid (LPA) in the systemic circulation

LPA, the product of the autotaxin (ATX) enzyme, has diverse roles in the vascular system, including the regulation of angiogenesis, remodeling, atherothrombosis and blood pressure. In the current project, we aimed to compare the vasoactive effects of saturated and unsaturated LPA species on the vascular tone and to identify their signal transduction. Since vascular diseases are more common in the elderly, we also aimed to observe the age-related changes of the 18:2 LPA induced vasoconstriction.

In aortic segments isolated from young and middle-aged (8 and 32 weeks old, respectively) wild-type (WT) and knock-out (KO) mice the vasoactive effects of different LPA species were determined with wire myography. To compare the LPA induced signal transduction in the two age groups general contractility and TXA_2 receptor sensitivity were tested by examining phenylephrine (PE) and U-46619 dose-response relationship, respectively. Expression profile of LPA_{1-3} receptors were demonstrated by qPCR in the VSM cells.

First, we assessed the vasoactive effects of the different LPA species in PE precontracted, endothelium-intact thoracic aorta segments. We investigated the 14:0, 16:0, 18:0 and 20:0 saturated LPAs. The 14:0 and 16:0 LPAs were able to elicit significant vasorelaxation, which was diminished in the vessels prepared from LPA_1-KO mice, suggesting that the effect is mediated by the LPA1 receptor. 18:0 and 20:0 LPAs did not elicit vasorelaxation.

Next, the vasorelaxant activity of 18:1, 18:2, 18:3 and 20:4 LPA was tested. 18:1 LPA elicited marked vasorelaxation, however with increasing the number of double bonds the relaxation decreased and became more transient. Surprisingly in the case of poly-unsaturated LPAs after the relaxation the vascular tone did not stabilizes at the level of the precontraction, as seen in the case of 18:1 LPA, but an additional contraction appeared. To identify the receptor responsible for the vasorelaxation, we tested the effect of the unsaturated LPAs in aortic segments isolated from LPA_1-KO mice. Unsaturated LPAs failed to induce vasorelaxation in vessels prepared from LPA_1-KO animals, suggesting that these LPAs elicit vasorelaxation via LPA_1 receptor as well.

We have previously reported that LPA_1 receptor activation can evoke both vasorelaxation and vasoconstriction. We hypothesized that in the case of endothelium intact aortic segments, we see the superimposition of these two opposite effects on the vascular tone. To examine the relaxant activity alone, the

LPA induced constrictor response had to be inhibited, therefore we applied the 18C LPAs to vessels treated with 10 μM indomethacin. When comparing the maximal elicited vasorelaxation induced by these LPAs, only the 18:3 LPA induced vasorelaxation was significantly increased in the COX inhibited aortic segments. However, analyzing the area over curve of the 18C LPA induced vasorelaxation within 5 minutes after administering the LPAs, vasorelaxation induced by both polyunsaturated LPA species was notably increased in the presence of indomethacin. No significant difference was detected in the relaxant activity of the investigated C18 LPAs in vessels treated with indomethacin, indicating that the cause of the acyl chain dependent differences in vasoactivity may be related to alterations in their constrictor capacity. Therefore, our next aim was to analyze the vasoconstrictor effects of LPAs.

As in our previous study using a synthetic LPA analogue, vasoconstriction induced by natural LPAs was significantly higher in AA segments compared to TA segments, therefore in this part of the study LPA species were applied on the resting tone of endothelium-denuded AA segments. Among the saturated LPAs (14:0, 16:0, 18:0 and 20:0 LPA) only the 14:0 LPA had constrictor activity. Vasoconstriction induced by unsaturated LPAs (18:1, 18:2, 18:3 and 20:4 LPA) had an increasing trend in parallel with the level of unsaturation. Dose-response curve fitting showed both increased efficacy and potency of the constrictor activity of poly-unsaturated LPA species (18:2, 18:3, and 20:4 LPA).

Next, we examined the constrictor effect of those LPA species, which had considerable constrictor activity, in AA segment isolated from LPA_1-KO mice. Vasoconstriction induced by 14:0 and 18C LPAs was completely abolished in the vessels prepared from LPA_1-KO mice. In contrast, in the aortic segments of LPA_1-KO mice, a significant proportion of vasoconstriction elicited by 20:4 LPA was preserved, indicating that another signaling pathway is involved in its constrictor effect. To gain better understanding of the structure-activity relationship of vasoconstriction, for further analyses we only investigated unsaturated 18C LPA species, as they evoke remarkable constriction, entirely mediated by LPA_1 receptor. Inhibiting COX with indomethacin, vasoconstriction evoked by unsaturated 18C LPA completely disappeared. As COX activation leads to the release of the potent vasoconstrictor, thromboxane, we aimed to measure the released TXB_2, which is a stable metabolite of TXA_2, in the supernatants of vessels exposed to 18C LPAs. Polyunsaturated 18:2 and 18:3 LPAs increased the TXB_2 production of the aortic segments, but not 18:1 LPA, suggesting the role of prostanoids in the increased constrictor effect. As COX activation is closely linked to the Gi protein signaling pathway, we investigated the participation of the G_i protein in the constrictor activity of the 18C LPAs. Mice were treated with PTX intraperitoneally for 5 days. Average contraction induced by 18:2 and 18:3 LPA was significantly decreased in the vessels isolated from mice treated with PTX compared to the aortic segments of mice treated with vehicle.

To get a better insight of the molecular mechanism underlying both the relaxant and constrictor activity, next we measured the intracellular Ca^{2+} signal after the administration of 18C LPAs in primary endothelial and vascular smooth muscle cell (VSMC) cultures. Endothelial cells showed a marked intracellular Ca^{2+}-increase when stimulated by 18C LPAs. In contrast to the endothelial cells, VSMCs exhibited negligible Ca^{2+} signal, suggesting that there are cell specific differences in the signaling of these LPAs, and raises further questions about the exact signaling mechanism underlying LPA_1-mediated thromboxane release and vasoconstriction.

Taken together, different naturally occurring LPA species have very different vasoactive effects. Interestingly, all these effects are mediated by the activation of LPA_1 receptor, suggesting that there might be cell specific differences in the signaling pathways. Shorter chain, saturated LPAs have a weak relaxing, and negligible constrictor effect, but as the chain becomes longer, these effects disappear. On the other hand, unsaturated LPAs have higher potency to evoke both the vasorelaxation and the vasoconstriction. This is in accordance with the literature data, as polyunsaturated LPA species might be stronger agonists of the LPA_1 receptor. Regarding the endothelial effects of the investigated polyunsaturated LPAs, their vasorelaxant activity decreased with the degree of unsaturation, but this seems not to be due to their ability to induce vasorelaxation, but rather due to a counteracting vasoconstrictor activity appearing only when polyunsaturated LPAs were tested. This is also supported by the Ca^{2+} measurement data in endothelial cells. We found that only polyunsaturated LPA species can evoke thromboxane production in the thoracic aorta, but, interestingly, this effect is not due to increased intracellular Ca^{2+} release by these LPA species in the smooth muscle cells. In conclusion, polyunsaturated LPA species have strong vasoconstrictor activity, due to their ability to increase COX mediated thromboxane release. This constriction is present even in endothelium intact aortic segments, where it counteracts LPA-mediated vasorelaxation, but is particularly interesting in case of endothelial injury and platelet activation where polyunsaturated LPAs can contribute to the progression of vasospasm via initiating thromboxane-mediated signaling.

Interestingly, 18:2 LPA mediated vasoconstriction was increased in the aortae of the 32-week old mice. There was no difference between the two age groups neither in the expression of LPA_1 receptor nor in the PE and U-46619 dose-response curves. 18:2 LPA mediated constriction was diminished in vessels of both the middle-aged and young COX1-KO animals.

Based on the results described above in detail, we further analyzed the signaling mechanism of the LPA induced vasoconstriction. For these experiments, 18:2 LPA was chosen, as it is one of the most abundant form of LPA under both physiological and pathophysiological conditions. As in the previous part of the study we did not see considerable intracellular Ca^{2+} increase upon LPA treatment in isolated VSMC, we started to do measurements with confocal wire myography. This technique is suitable to visualize the Ca^{2+}-changes and vascular tone simultaneously in isolated

vessels. First, we removed both the endothelium and adventitia, and loaded the remaining smooth muscle layer with Fura-2AM. Surprisingly, removal of the adventitia abolished the 18:2 LPA induced vasoconstriction and the elicited Ca^{2+}-response was minimal. On the other hand, phenylephrine- and potassium-induced contraction and Ca^{2+} signals were clearly visible, indicating the integrity of the smooth muscle layer and its ability to constrict upon stimulation. Interestingly, when only the adventitia was pulled on the pins of the confocal myograph, a marked Ca^{2+}-signal was detectable upon 18:2 LPA administration.

This difference was also present, when isolated vascular smooth muscle cells were compared to isolated adventitial cells. In a primary isolated vascular smooth muscle cell culture, 18:2 LPA elicited only minimal changes in the intracellular Ca^{2+}. The purity of the culture was verified by α-SMA (smooth muscle actin) staining. A mixed culture of isolated adventitial cells was thereafter tested. In some of the cells, there was a prominent Ca^{2+}-signal. After the cells were fixed and stained, we concluded that only those cells showed the Ca^{2+}-signal, which were positive for LPA_1 receptor but negative for the smooth muscle marker.

Thereafter we aimed to further analyze the localization of LPA_1 receptor in the mouse aorta. First, we demonstrated that the antibody of our choice is indeed specific for LPA_1 receptor as LPA_1 immunostaining was completely absent in the aorta prepared from LPA_1 KO mouse. En face staining of the aorta showed that the tunica adventitia expresses the LPA_1 receptor, while the tunica media does not.

We also confirmed the importance of the tunica adventitia in the vasoconstrictor effect of 18:2 LPA, as well as its role in the thromboxane production upon 18:2 LPA treatment. In accordance to this, we were able to detect significantly higher LPA_1 expression with qPCR when the adventitia was not removed from the aorta. Therefore, we concluded that a yet unidentified cell type of the adventitia mediates the vasoconstrictor effect of LPA.

Vascular effects of LPA in mouse models of dyslipidemia and type II diabetes

In order to examine the potential changes of vascular reactivity to LPA in cardiovascular diseases, we performed experiments in two different mouse strains of accelerated atherosclerosis. The first model was the widely used ApoE deficient strain. Mice with this genetic modification have marked increase in total plasma cholesterol levels and consequently exhibit accelerated atherogenesis. We tested the general vascular reactivity, and the vasoconstrictor effect of 18:2 LPA in aged ApoE KO male and an age matched control mice. Vessels of ApoE deficient mice showed decreased endothelium dependent vasorelaxing capacity and increased LPA induced vasoconstriction compared to the control vessels.

The same increased vasoconstriction to 18:2 LPA was not detectable in db/db diabetic mice, another model of accelerated atherogenesis. On the other hand, we found several differences in these mice related to lysophospholipid homeostasis.

Plasma level of lysophosphatidylcholine (LPC), the main precursor of LPA synthesis was elevated in the db/db mice. Autotaxin, the enzyme which produces LPA from LPC – showed higher expression levels in the subcutaneous and periaortic adipose tissue of the diabetic mice compared to control. According to literature data, the majority of plasma ATX is originated from adipose cells, and ATX can attach to the surface of endothelial cells through activated integrin receptors resulting in LPA production in the close proximity of its receptors. Given that db/db mice are obese, circulating ATX levels may be extremely high. Our finding raises the possibility that, combined with high substrate levels, increased ATX could lead to increased local production of LPA, contributing to the accelerated atherogenesis seen in diabetes.

As we found that vessels of ApoE deficient mice showed increased LPA induced vasoconstriction compared to the control vessels we aimed to analyze its involvement in the development of endothelial dysfunction in atherosclerosis. Therefore, we challenged the ApoE KO mice with 'Western-type' diet, and evaluated the potential endothelium protective effect of the ATX inhibitor GLPG1690 applied in vivo. We performed several preliminary experiments in ApoE mice to set the length of the diet, in which the thoracic aorta shows the earliest signs of vascular dysfunction with significant impairment of ACh dependent vasodilation but minimal or absent plaque formation. We sacrificed 2 mice every second week to test the endothelial function, but unfortunately, endothelial dysfunction did not develop in the first 12 weeks after initiation of the diet. Neither ACh-induced vasorelaxation, nor its nitric oxide mediated component decreased during the investigated period. We have also unsuccessfully tried LDL receptor KO mice, as a frequently used another model of accelerated atherogenesis. Interestingly, in spite of the unaltered endothelial function, atherosclerotic plaque formation was clearly detectable with Oil Red staining in both animal models.

Molecular mechanisms of the endothelial dysfunction induced by lysophoshatidylcholine (LPC)

Lysophosphatidylcholine (LPC) is a component of the oxidized low-density lipoprotein that plays a major role in the development of atherosclerosis. According to the literature, LPC impairs endothelium-dependent vasorelaxation by decreasing the bioavailability of NO, however the underlying mechanisms are not completely understood. LPC can be converted into LPA by the lysophospholipase autotaxin (ATX). We aimed to examine the involvement of ATX and LPA in LPC-induced endothelial dysfunction. In thoracic aorta segments isolated from adult male wild-type (WT) C57/Bl6 as well as LPA_1, LPA_2, LPA_4, LPA_5 receptor KO mice the effect of 18:1 LPC or 18:1 LPA on ACh-induced, endothelial NO-dependent vasorelaxation was tested using wire myography. To test the effect of ATX inhibition on the LPC induced endothelial dysfunction we used the selective ATX inhibitor GLPG 1690. We found that 18:1 LPC significantly reduces the ACh-dependent vasorelaxation of WT mice which could be partially prevented by inhibition of ATX. Therefore, we concluded that LPC mediates its deleterious effects as converted to LPA by ATX.

In order to further prove our hypothesis, we tested the effect of LPC on the vessels of different LPA receptor KO mice. LPC evoked endothelial dysfunction was unaltered in LPA_1, LPA_2, and LPA_4 KO aortic segments, whereas it was significantly decreased in LPA_5 KO. These observations suggest that the locally produced, LPC-derived LPA activates LPA_5 receptors on site, thus contributing to the impairment of endothelial function. Additionally, we also examined the LPA receptor and ATX expression profile in aortic tissue isolated from WT and LPA_5 KO mice using quantitative real-time PCR. Our data showed that *Lpar5* deletion did not significantly affect the expression of LPA_1, LPA_2, LPA_3, LPA_4, LPA_6 receptors and ATX as no significant differences in mRNA expression rate were detected relative to WT.

In the next phase of the study, we intended to examine further the molecular mechanisms involved in this phenomenon. As both LPC and LPA are known to induce prostanoid-dependent signaling, we tested the involvement of this pathway. The effect of LPC developed in both COX-1 and TP receptor KO mice implying that the COX-1-TP axis is unlikely to be involved. In contrast, the effect of LPC was significantly decreased in the presence of superoxide dismutase (SOD) and LPC evoked a marked increase in H_2O_2 levels in the aortic tissue of WT mice. Interestingly, in LPA_5 KO vessels the beneficial effect of SOD was absent. Furthermore LPA_5 deficiency also attenuated LPC-induced H_2O_2 generation.

As we have also shown that reactive oxygen species (ROS) production contributes to the development of endothelial dysfunction elicited by LPC we aimed to show the increased ROS production directly by dihydroethidium (DHE) staining after treatment with LPC, and evaluate whether it can be attenuated by GLPG1690. DHE causes red fluorescence in the presence of intracellular superoxide. First, we performed the staining of the whole thoracic aorta and tried to evaluate the DHE signal in *en face* preparations. However, we were not able to quantify the increase in the DHE signal after LPC treatment, mostly because of the high background fluorescence of the aortic smooth muscle cells. Therefore, we tried DHE staining in human umbilical venous endothelial cells (HUVECs). LPC treatment in HUVEC cells elicited a significant increase in the DHE signal, which was surprisingly not sensitive to GLPG1690 treatment. There are several possible explanations for this finding, one of which is that the source of ROS in the whole aorta is not the endothelium. This latter is also supported by our finding, that in myographic experiments, the cell impermeable SOD was also able to reduce the LPC effect.

In conclusion, we have shown that the development of LPC-induced impairment of endothelium-dependent vasorelaxation requires the conversion of LPC to LPA by the ATX enzyme. This locally formed LPA appears to activate LPA_5 receptor, triggering signaling pathways that lead to an elevated production of ROS and subsequent endothelial dysfunction. These results show, that ATX and LPA have an important role in LPC-induced endothelial dysfunction.

Effects of LPA in the murine coronary circulation

Unsaturated LPA species are released reportedly in acute coronary syndrome. Therefore, our next aim was to describe the effects of 18:1, 18:2 and 18:3 LPA on the coronary flow (CF) of isolated murine hearts and to identify the signaling pathways involved. qPCR analysis verified the expression of each known LPA receptor (LPA_{1-6}) in mouse coronary arteries. Administration of 18:1, 18:2 and 18:3 LPA to the perfusion line of Langendorff perfused hearts of WT male mice caused a substantial CF reduction (up to 35%) which resulted in the drop of left ventricular developed pressure. This effect of LPA also developed in LPA_1 and LPA_2 deficient mice and in the presence of LPA_3 antagonists (Ki16425 and VPC32183). However, administration of the LPA_4 antagonist BrP-LPA abolished the effect. In accordance, LPA_4-KO mouse hearts were partly resistant to the CF effect of LPA. In addition, smooth muscle specific deletion of $G\alpha_{q/11}$ proteins did not influence, whereas that of $G\alpha_{12/13}$ diminished by 50% the CF reduction. Rho-kinase (ROCK) inhibition (Y27632) abolished the effect of LPA on CF. Moreover, deletion of endothelial NO synthase enhanced, whereas inhibition of endothelin A receptor by BQ123 diminished the response of coronaries to LPA.

In conclusion, polyunsaturated LPAs appear to have strong, age-dependent vasoconstrictor activity in the systemic circulation. In addition, unsaturated 18-LPA species are strong vasoconstrictors in the coronaries as well. LPA_4 receptors, endothelin-1 and the $G\alpha_{12/13}$ protein - ROCK signaling pathway are involved in mediating coronary vasoconstriction. This process might have relevance in acute coronary events when a large amount of unsaturated LPA is released in the coronary system due to platelet activation and plaque rupture.

Effects of spnigosine-1-phosphate (S1P) on coronary flow and heart function in mice

To better understand the effects of S1P on the coronary circulation, we conducted *ex vivo* experiments in isolated murine hearts mounted on the Langendorff-system. Left ventricular pressure and coronary flow (CF) were continuously monitored. After equilibration, S1P or its vehicle was infused to the perfusion line for 5 minutes. S1P induced CF reduction immediately after the onset of infusion and continued progressively during the 5 min of administration. Interestingly, during the 20-min wash-out period, CF did not return to the baseline level and remained at a significantly lower value. Reduction of the CF was accompanied by compromised left ventricular contractile performance, which is indicated by a drop in left ventricular developed pressure and by markedly decreased +dLVP/dtmax, and -dLVP/dtmax values. The vehicle did not affect either CF or other measured heart function parameters.

Earlier studies indicated that S1P might affect coronaries via $S1P_2$ and $S1P_3$ receptors. In order to identify which S1P receptors participate, we applied S1P in the presence of selective $S1P_2$ inhibitor JTE-013 and the selective $S1P_3$ inhibitor

TY52156. In the presence of these inhibitors reduction of coronary perfusion and decline in heart function were diminished. Simultaneous inhibition of $S1P_2$ and $S1P_3$ abolished the effect of S1P on CF. The contribution of $S1P_1$ receptor was assessed after its smooth-muscle specific deletion. Interestingly, this resulted in the enhancement of the S1P-induced coronary effect.

In further studies we perfused S1P into the isolated hearts of $S1P_2$ and $S1P_3$ KO mice following the experimental protocol described above. The CF-reducing effect of S1P developing in $S1P_2$ deficient mice was similar to that of WT littermates. The drop of the left ventricular developed pressure was also similar in the two groups, with no statistically significant difference. In $S1P_3$-KO hearts, the CF-reducing effect of S1P was markedly diminished compared to WT mice. The decrease in left ventricular contractile performance upon S1P infusion was also attenuated in $S1P_3$-KO mice: the maximal drop in left ventricular developed pressure was significantly reduced compared to WT controls. In conclusion we established that $S1P_2$ has only a minor role, whereas $S1P_3$ is a key determinant in the CF reducing effect of S1P.

Further experiments were conducted to identify the G-proteins participating in the intracellular signaling. Smooth muscle-specific deletion of $G\alpha_{q/11}$ did not influence the S1P effect. However, pharmacological inhibition of the $G\alpha_{12/13}$ coupled ROCK enzyme with Y-27632 diminished S1P-mediated flow reduction. The $G\alpha_{i/o}$ was studied in the hearts of pertussis toxin pretreated mice. In these hearts enhanced CF reduction was observed upon S1P infusion.

The potential participation of endothelial vasoactive mediators was also assessed. Genetic deletion of endothelial NO-synthase, and pharmacological inhibition of endothelin A receptor by BQ123 did alter the CF response to S1P.

In conclusion, the CF reducing effect of S1P is mediated by $S1P_2$ and $S1P_3$ receptors, presumably via redundant pathways. The $G\alpha_{12/13}$ coupled ROCK pathway may have a major role in the signaling. An S1P-dependent coronary dilator mechanism has also been identified. This may be mediated by a $S1P_1$ receptor. Interestingly, $G_{i/o}$ protein seems to play a role in this vasodilator response. Based on literary data we hypothesize the role of $G_{i/o}$ dependent COX2 activation, and PGI_2 release in this effect.

Role of myocardial $S1P_3$ receptor activation in I/R injury

S1P has been attributed with cardioprotective effects against ischemia-reperfusion (I/R) injury by several research groups. We investigated the effects of potential $S1P_3$ receptor activation during I/R in Langendorff-perfused mouse hearts. WT and $S1P_3$-KO hearts were exposed to an I/R protocol, CF and myocardial function were monitored during reperfusion. CF did not differ significantly between the WT and $S1P_3$-KO mice. In contrast, parameters describing myocardial performance showed marked differences. The lack of $S1P_3$ resulted in a far worse postischemic functional recovery as evidenced by the drop of the left ventricular developed pressure,

decreased +dLVP/dtmax, and -dLVP/dtmax, and elevated left ventricular diastolic pressure.

These results indicate that $S1P_3$ receptors play a beneficial role in preventing ischemia-induced myocardial dysfunction, most probably by activation from S1P generated locally by the tissues of the ischemic heart. However, this myocardial S1P release did not induce $S1P_3$-mediated coronary vasoconstriction as observed in the previous experiments with intravascular S1P administration. Lack of $S1P_2$ receptors did not influence any of these functional parameters in this I/R model.

Effects of preischemic intravascular S1P exposure on I/R injury

Preischemic S1P treatment has also been reported to decrease infarct size in ex vivo experimental models. We investigated the role of intravascular S1P by administering S1P to Langendorff-perfused mouse hearts before I/R at a concentration of 10^{-6} M for 5 min. Under these conditions, CF returned to a significantly higher value during reperfusion in the $S1P_3$-KO hearts indicating $S1P_3$-mediated coronary vasoconstriction. Postischemic myocardial function failed to return during the reperfusion without any difference between the two groups. In order to determine the effects of S1P infusion on postischemic CF and cardiac performance, results obtained by the two experimental protocols were compared. S1P-exposed WT hearts showed a marked reduction in post-ischemic functional myocardial recovery as compared to WT or $S1P_3$-KO hearts without S1P administration. Furthermore, the difference in the functional parameters between WT and $S1P_3$-KO hearts was not statistically significant.

Vasoactive effect of LPA and S1P on human coronary arteries

We have set up the method of isolated human coronary artery wire myography to gain insight into the effects of lysophospholipids in the human vasculature, and tested epicardial coronary arteries prepared from explanted hearts as part of a biobanking process at the Semmelweis University Heart and Vascular Center. 18:2 LPA induced relaxant responses human coronary arteries with intact endothelial layer. On the other hand, after mechanical removal of the intima, vasoconstriction was detectable, but interestingly, this only appeared in vessels isolated from patients with coronary artery disease (CAD). We were able to inhibit the constriction with the $LPA_{1/3}$ receptor antagonist Ki16425 indicating that the receptor involved in the signalization is the $LPAR_1$ or $LPAR_3$.

In another experimental setup, we tested the effects of another lysophospholipid mediator, S1P. In 6 patients with heart failure due to primary dilatative cardiomyopathy (DCM) and no signs of CAD, S1P was able to evoke an unexpectedly large coronary vasorelaxation (comparable, or even larger than that of bradykinin, a standard vasorelaxant in the coronary circulation). Altogether, 33 epicardial artery segments were tested from 6 patients, 18 of them were controls, 6 segments were pretreated with $S1P_3$ receptor inhibitor TY52156 with no change in the vasorelaxing effect of S1P. Another 9 segments were pretreated with $S1P_1$

receptor inhibitor W146 (10 μM), which completely abolished the S1P induced vasorelaxation.

Our results indicate that both LPA and S1P have significant effects on the tone of human coronary arteries ex vivo. The vasoconstrictor effect of LPA appearing exclusively in vessel segments prepared from patients suffering from CAD may indicate that LPA homeostasis is disturbed in this disease, possibly due to changed receptor expression or signalization. It is also possible, that enzymes (lipid phosphate phosphatase, LPP3) capable of hydrolyze LPA before it could act on its receptors are less available. This would coincide with literature data, as LPP3 coding gene locus is associated with CAD susceptibility, shown by human genome wide association studies. In contrast to LPA, S1P appears to induce vasorelaxation mediated by $S1P_1$ receptors.

LPA suppresses HLA-DR expression in melanoma: a potential immune escape mechanism involving LPA_1 and DR6 receptor-mediated IL-10 release

Melanoma is the most aggressive type of skin cancer. While immune checkpoint inhibitors (ICIs) are a promising treatment for metastatic melanoma, approximately 50% of patients do not respond well to them. Recently, elevated expression of human leukocyte antigen-DR (HLA-DR) in tumors has been shown to predict better prognosis and response to ICIs. In the present study, we found that lysophosphatidic acid (LPA), a bioactive lipid mediator, suppresses HLA-DR expression in melanoma cells by upregulating death receptor 6 (DR6) expression. DR6 is inducibly expressed in tumor cells and regulates diverse cellular functions, including cytokine release. Our results reveal that activation of the LPA_1 receptor via G_i-coupled signaling elicits NF-kB-mediated transcriptional upregulation of DR6 in human melanoma cells. In turn, DR6 upregulates the expression and release of interleukin-10 (IL-10), resulting in diminished HLA-DR expression. Furthermore, we found significant correlation between expression of LPA_1, DR6 and IL-10 in human melanoma tissue and association between increased LPA_1 expression with reduced effectiveness of ICI therapy. These data highlight that the LPA_1-DR6-IL-10 autocrine loop could constitute a novel mechanism used by tumor cells to evade immunosurveillance by decreasing HLA-DR expression.

Characterization of native and human serum albumin-bound LPA Species and their effect on the viability of mesenchymal stem cells

We aimed to assess the complex formation between human serum albumin (HSA) and LPA in aqueous solutions and to determine the effect of the most abundant, albumin-bound 16:0, 18:1, and 18:2 LPA species on the proliferation and migration of human bone marrow-derived mesenchymal stem cells (hBM-dMSCs).

To evaluate if the complex formation occurs between LPA and HSA, we investigated structure-related chemical changes with the use of Fourier-transform infrared (FTIR) spectroscopy. This method can be used to detect complex formation between LPA and HSA. The IR spectra were assessed for the three, physiologically most abundant

16:0, 18:1, and 18:2 LPA derivatives. According to our results, the spectral changes might indicate the binding of LPA species to HSA. Next, we performed XTT measurements to investigate the possible cytotoxicity and to determine the effects of 18:1, 18:2, and 16:0 LPA on the proliferation of hBM-dMSCs. 18:1 LPA in 1, 3, and 10 μM concentrations significantly increased cell proliferation compared to the control group, but solely when administered in the presence of HSA. In addition, 18:2 LPA significantly enhanced the proliferation of hBM-dMSCs in combination with HSA in 1, 3, and 10 μM and when examined alone in 3 and 10 μM concentrations. A significant elevation in the cell proliferation was caused by 0.3, 1, 3, and 10 μM 16:0 LPA treatment, exclusively in combination with HSA. To investigate if 18:1, 18:2, or 16:0 LPA influence the migration of the hBM-dMSCs, wound healing assay experiments were performed. Cell migration analysis showed no significant enhancement after LPA treatment, with or without HSA. Thus, the observed cell proliferative effect of LPA treatment is not directly associated with the enhanced migration of hBM-dMSCs.

Enhancement of sphingomyelinase-induced endothelial nitric oxide synthase-mediated vasorelaxation in a murine model of type 2 diabetes

Sphingolipids, derived from sphingomyelin metabolism, have been implicated as important mediators in the physiology and pathophysiology of the cardiovascular system. Sphingomyelinase (SMase) catalyzes the conversion of sphingomyelin to phosphoryl choline and ceramide, the latter is the precursor of other sphingolipid mediators, including ceramide-1-phosphate (C1P), sphingosine (Sph), and S1P. Normally, sphingomyelin (SM) represents about 10-20% of the lipids in the plasma membrane, mostly residing in the outer leaflet. However, most of these are found in the caveolae, and SMase is thought to be a regulator of lipid microdomains. In the vasculature, SMases are implicated in the regulation of vascular tone and permeability as well as in causing atherosclerotic lesions and vascular wall remodeling. SMase enzymes are reportedly upregulated in certain cardiovascular and metabolic disorders such as type 2 diabetes mellitus (T2DM). Although neutral Smase (nSMase) has been reported to induce a wide range of changes in the vascular tone, depending on the species, vessel type, and experimental conditions, relatively little is known about the effects of sphingolipids on vascular functions in T2DM. Therefore, we analyzed the effects of SMase on vascular tone under diabetic conditions in order to elucidate the signaling mechanisms involved.

First, we verified the general metabolic and vascular phenotype of T2DM mice tested in the study. The body weight increased almost 2-fold, whereas blood glucose levels increased 3-fold in db/db mice as compared to non-diabetic control littermates. Furthermore, the serum phosphoryl choline level was also significantly increased in the diabetic group, which is consistent with the reported enhancement of SMase activity in type 2 diabetes. Vessels of db/db animals showed marked endothelial dysfunction indicated by the impairment of the dose-response relationship of ACh-induced vasorelaxation. These results confirm the T2DM-like metabolic and vascular

phenotypes in db/db mice and suggest the *in vivo* enhancement of SMase activity as well.

Next, we determined the effect of nSMase on the active tone of control and db/db vessels. After phenylephrine (PE)-induced precontraction, 0.2 U/mL nSMase elicited additional contraction in control vessels that reached its maximum at 7.2 min before relaxing back to the pre-SMase level by the end of the 20-min observation period. In contrast, nSMase in db/db vessels elicited completely different responses. Surprisingly, after a marked initial relaxation during the first 5 min, the tone of the db/db vessels remained in a relaxed state below the level of the initial tension.

Our next aim was to differentiate the constrictor and relaxant components of the vascular tension changes in response to nSMase. According to literature data, prostanoids acting on TP receptors have been implicated in mediating the vasoconstrictor effect of SMase. Therefore, we hypothesized that thromboxane prostanoid (TP) receptors also mediate the nSMase-induced vasoconstriction in our murine aorta model. Blockade of TP receptors not only abolished the vasoconstriction, but also converted it to a transient vasorelaxation in control vessels. This relaxation was even more strongly enhanced and prolonged in the db/db group. This finding was very surprising in light of the diminished ACh-induced vasorelaxation that we had observed in db/db animals, and was not consistent with the large body of literary data indicating diminished endothelium-dependent vasorelaxation in T2DM.

Finally, we aimed to analyze the mechanism of the enhanced nSMase-induced vasorelaxation in vessels of db/db mice, whether it is due to the enhancement of eNOS-mediated vasorelaxation or to the onset of an NO-independent mechanism. After coadministration of eNOS inhibitor and TP receptor blockers, we could not detect considerable change in vascular tension neither in control, nor in db/db aortas upon nSMase treatment.

Taken together, administration of nSMase induces TP receptor-mediated vasoconstriction and eNOS-mediated vasorelaxation in murine vessels. In spite of endothelial dysfunction in db/db mice, the vasorelaxant effect of nSMase is markedly augmented. A possible mechanism responsible for enhanced NO generation in T2DM can be the SMase-mediated disruption of sphingomyelin in endothelial lipid rafts, as this could interfere with the caveolar structure and induce the detachment of eNOS from caveolin-1, leading to high amounts of NO released from the endothelium of db/db vascular rings. An intriguing interpretation of our finding is that retraction of eNOS in sphingomyelin-rich microdomains of the endothelial plasma membrane could contribute significantly to the development of vascular dysfunction in T2DM.

Adaptation of the cerebrocortical microcirculation to unilateral carotid artery occlusion

Carotid artery stenosis (CAS) is recognized as a significant risk factor for vascular cognitive impairment (VCI). The impact of CAS on cerebral blood flow (CBF) within the ipsilateral hemisphere relies on the adaptive capabilities of the cerebral circulation. We aimed to test the hypothesis that the impaired availability of NO compromises CBF homeostasis after unilateral carotid artery occlusion (CAO). In wild-type animals, a rapid CoBF decrease was observed in the ipsilateral frontal, parietal, and temporal regions after CAO. This observation suggests that the existing macrovascular connections (i.e., the arteries of the Willis circle) are not sufficient to compensate immediately and completely for the occlusion of one CCA and that active cerebral vasodilation is required to adapt cerebrocortical circulation to the altered hemodynamic situation. The decreased blood flow in the frontal and parietal regions can be explained by a stealing effect through pial anastomoses between the territories of MCA and AACA. These anastomoses have a crucial role in the adaptational process after CCA occlusion, as the blood from the frontoparietal regions is drained via pial anastomotic vessels to the more ischemic temporal cortex of the ipsilateral hemisphere (“steal phenomenon”). Surprisingly, genetic deletion of NOS3 failed to influence cerebrovascular adaptation to unilateral carotid artery occlusion in mice, possibly due to the elevated blood pressure in NOS3 KO animals.

In contrast NOS1 plays an important role in the adaptational process, as mice lacking neuronal nitric oxide synthase (NOS1 KO) showed increased tortuosity of pial collateral vessels, and double knockout mice of NOS1 and endothelial nitric oxide synthase (NOS1/3 DKO) exhibited impaired cerebrocortical blood flow adaptation to CAO, particularly in the subacute phase. The more pronounced impairment observed in NOS1/3 DKO mice indicates a synergistic role of NO derived from NOS1 and NOS3 in maintaining cerebrovascular homeostasis. Furthermore, pharmacological inhibition of NO synthesis by L-NAME resulted in severe alterations in CBF adaptation to CAO. Animals treated L-NAME exhibited marked and prolonged hypoperfusion in both the ipsilateral and contralateral hemispheres in the acute phase, confirming the crucial role of NO in compensatory mechanisms following CAO. Interestingly, acute pharmacological inhibition of NO synthesis had more severe consequences in the acute phase of adaptation, whereas genetic deletion of NOS1/3 mostly compromised the CBF recovery during the subacute phase. We propose that this difference may be related to compensatory vasoregulatory mechanisms upregulated during chronic NO deficiency and probably explains the milder hypertension in NOS KO compared to L-NAME-treated mice. These compensatory mechanisms may support the CBF recovery during the acute phase of adaptation to CAO, resulting in a less severe phenotype of NOS1/3 DKO than L-NAME-treated mice. In the subacute phase, however, the unfavorable morphological change (increased tortuosity) of the leptomeningeal collaterals and

lack of NO-mediated vasodilation together may be responsible for the prolonged hypoperfusion of the brain in NOS1/3 DKO mice.

Signal transduction pathways of prostanoids and isoprostanes in urinary bladder smooth muscle

Our aim was to examine the effects and the signal transduction pathways of prostanoids and isoprotanes in the urinary bladder smooth muscle. Prostaglandin E_2 (PGE_2) and prostaglandin $F_{2\alpha}$ ($PGF_{2\alpha}$), as well as the isoprostane 8-epi-PGE_2 and 8-iso-$PGF_{2\alpha}$ evoked contraction in isolated mouse urinary bladder strips. The effect of the prostanoids was decreased, and the effect of the isoprostanes was abolished in the strips of thromboxane prostanoid receptor (TP) KO mice, suggesting that the effect of the prostanoids is mediated partially, whereas that of the isoprostanes mainly by the TP. Smooth muscle specific deletion of $G\alpha_{12/13}$ proteins and ROCK inhibition by Y-27632 decreased the contractions. Smooth muscle specific deletion of $G\alpha_{q/11}$ proteins also decreased the contractions which were abolished completely in the presence of Y-27632.

In conclusion, the contractile effects of the examined prostanoids and isoprostanes are mediated mainly by the TP receptor and linked to the $G_{q/11}$ and to the $G_{12/13}$-ROCK intracellular signaling pathways in the murine urinary bladder. The $G_{12/13}$-ROCK signaling pathway may provide a novel pharmacological target in the treatment of overactive bladder.

Signaling pathways mediating bradykinin-induced contraction in murine and human detrusor muscle

Bradykinin (BK) has been proposed to modulate urinary bladder functions and implicated in the pathophysiology of detrusor overactivity. We aimed to elucidate the signaling pathways of BK-induced detrusor contraction, with the goal of better understanding the molecular regulation of micturition and identifying potential novel therapeutic targets of its disorders.

Experiments have been carried out on bladders isolated from wild-type or genetically modified [smooth muscle-specific KO: $G\alpha_{q/11}$-KO, $G\alpha_{12/13}$-KO and constitutive KO: thromboxane prostanoid (TP) receptor-KO, cyclooxygenase-1 (COX-1)-KO] mice and on human bladder samples. Contractions of detrusor strips were measured by myography.

BK induced concentration-dependent contractions in both murine and human bladders, which were independent of secondary release of acetylcholine, ATP, or prostanoid mediators. B_2 receptor antagonist HOE-140 markedly diminished contractile responses in both species, whereas B_1 receptor antagonist R-715 did not alter BK's effect. Consistently with these findings, pharmacological stimulation of B_2 but not B_1 receptors resembled the effect of BK. Interestingly, both $G\alpha_{q/11}$- and $G\alpha_{12/13}$-KO murine bladders showed reduced response to BK indicating that simultaneous activation of both pathways is required for the contraction.

Furthermore, the ROCK inhibitor Y-27632 markedly decreased contractions in both murine and human bladders.

These results indicate that BK evokes contractions in murine and human bladders, acting primarily on B_2 receptors. $G\alpha_{q/11}$-coupled and $G\alpha_{12/13}$-RhoA-ROCK signaling appear to mediate these contractions simultaneously. Inhibition of ROCK enzyme reduces the contractions in both species, identifying this enzyme, together with B_2 receptor, as potential targets for treating voiding disorders.

Role and signaling of muscarinic receptors in detrusor muscle contraction

We aimed to analyze the role of the M_2 and M_3 muscarinic receptors and their corresponding heterotrimeric G proteins (G_i and $G_{q/11}$, respectively) in the regulation of detrusor function, concentrating on the interaction with the Rho-ROCK pathway. We demonstrated that the ROCK plays a pivotal role in the detrusor contraction induced by the muscarinic receptor agonist, CCh. Moreover, the CCh-induced contractions and RhoA activation are mediated by both the M_2 and the M_3 receptors according to the results gained from M_2-, M_3 and M_2/M_3-KO animals. In addition, the expression levels of other muscarinic receptors were not altered by the genetic deletion of M_2 and M_3 receptors indicating that no other muscarinic receptors contribute to the UBSM contraction induced by CCh. Furthermore, pharmacological inhibition of the ROCK enzyme had an additional inhibitory effect on the concentration-response curve of CCh in M_2- and M_3-KO mice. Interestingly, there was no change in the expression of the $ROCK_1$ enzyme in detrusor muscle from mice deficient in M_2 or M_3 receptors, however, the $ROCK_2$ expression was elevated in M_2/M_3 KO mice suggesting a compensatory upregulation of ROCK in the absence of both receptors. PTX treatment of WT mice shifted the concentration-response curve of CCh to the right parallel with a steep decrease in RhoA activation. The CCh-induced contractions were diminished in $G_{q/11}$-KO animals however, the RhoA activation did not change in mice deficient in $G_{q/11}$ compared to that of WT. These results indicate that muscarinic receptor-mediated RhoA activation is not mediated by $G_{q/11}$ but rather by G_i.

Appendices

Reprints of papers in the process of publication

International Journal of *Molecular Sciences*

MDPI

Article

Acyl Chain-dependent Vasoactive Effects of Lysophosphatidic Acid: Only Poly-unsaturated Species Induce Thromboxane A2-mediated Vasoconstriction

Krisztina Vén [1,2], Balázs Besztercei [1], Noémi Karsai [1,3], Jerold Chun [4], Gábor Tigyi [1,5], Zoltán Benyó [1,6] and Éva Ruisanchez [1, 6,*]

[1] Institute of Translational Medicine, Semmelweis University, Budapest, Hungary
[2] Semmelweis University, Department of Neurology, Budapest, Hungary.
[3] Division of Physiology, Pharmacology and Neuroscience, School of Life Sciences, Queen's Medical Centre, University of Nottingham, Nottingham, UK
[4] Sanford Burnham Prebys Medical Discovery Institute, La Jolla, California, USA
[5] Department of Physiology, University of Tennessee Health Sciences Center, Memphis, Tennessee, USA
[6] HUN-REN-SU Cerebrovascular and Neurocognitive Disorders Research Group, Budapest, Hungary
* Correspondence: ruisanchez.eva@med.semmelweis-univ.hu

Abstract: We have previously reported that 18:1 lysophosphatidic acid (LPA) can induce both vasodilation and vasoconstriction depending on the integrity of the endothelium. Platelet activation leads to the production of several poly-unsaturated LPA species, yet their vascular effects are largely unexplored.

We aimed to compare the vasoactive effects of seven naturally occurring LPA species, to elucidate their potential pathophysiological role in vasculopathies.

Vascular tone was measured using myography and thromboxane A_2 (TXA_2) release was detected by ELISA in the mouse aorta. The Ca^{2+}-signal of primary isolated endothelial cells was measured by Fluo-4 AM imaging.

Our results indicate that saturated LPAs have no significant effect on the vascular tone. Among unsaturated 18 carbon-containing (C18) LPAs (18:1, 18:2, 18:3), the most pronounced vasorelaxation is induced by the 18:1 LPA. However, after inhibition of cyclooxygenase (COX), these LPAs induced similar vasorelaxation, indicating that the vasoconstrictor potency differed among these species. Indeed, C18 LPAs evoked similar Ca^{2+}-signal in endothelial cells, whereas in endothelium-denuded vessels the constrictor activity increased with the level of unsaturation as was TXA_2 release in intact vessels. COX inhibition abolished the C18 LPAs induced vasoconstriction and TXA_2 release.

In conclusion, polyunsaturated LPAs have markedly increased TXA_2-releasing and vasoconstrictor capacity implying potential pathophysiological consequences in vasculopathies.

Keywords: lysophosphatidic acid, lysophosphatidic acid receptor 1, thromboxane, vasoconstriction

Citation: To be added by editorial staff during production.

Academic Editor: Firstname Lastname

Received: date
Revised: date
Accepted: date
Published: date

1. Introduction

Lysophosphatidic acid (LPA) is a bioactive lysophospholipid mediator found in all eukaryotic tissues and most biological fluids. LPA mediates and modulates several physiological effects ranging from the development of the nervous system, regulation of the immune response and pathophysiological events like neuropathic pain and fibrosis[1-4]. LPA also has roles in the vascular system, including regulation of angiogenesis,

vascular wall remodeling [5] and blood pressure [1, 6]. LPA refers to a family of phospholipids characterized by a glycerol backbone linked to a phosphate group and a fatty acid or fatty alcohol chain. Acyl-LPAs contain ester linkage between the glycerol backbone and the fatty acid, whereas in the alkyl-LPAs, correctly termed as alkyl phosphatidic acids, the fatty alcohol chain is linked with an ether bond. Acyl LPAs are more abundant, but the LPAR5, a potent activator of platelets prefers alkyl-LPA [7]. LPA species differ in the number of double bonds in the hydrocarbon chain. The acyl chain can be esterified to either the sn1 or the sn2 carbon in the glycerol backbone. Furthermore, the phosphate group can be linked to both the sn1 and the sn2 carbons in cyclic-phosphatidic acids [8].

Traditionally, the most widely investigated LPA type is the 18:1 LPA, although it is not the most abundant form in the biological fluids of vertebrates. In plasma, the concentration of LPA is approximately 50 nM, and the most common forms are LPA 18:2 > 20:4 > 16:0 > 18:1 [9]. Its concentration is elevated up to 5 μM in the serum, and the relative proportion of the LPA isoforms changes to 20:4 > 18:2 > 16:0 > 18:1 > 18:0 [10]. It is noteworthy that the amount of LPA is elevated in plasma of patients with acute coronary syndrome [11] and hypertension [12], particularly the levels of LPAs 18:2 and 20:4 [13]. During vascular injury or rupture of an atherosclerotic plaque, the ensuing platelet activation leads to the localized production of mainly polyunsaturated LPA species (PU-LPA) dominated by 18:2 and 20:4 species [14].

LPA evokes its effects mainly via six G-protein-coupled receptors, LPAR1-6 and the peroxisome proliferator-activated receptor-γ. In the vessel wall LPAR1 receptors are present in both the endothelium and the vascular smooth muscle [15, 16]. LPAR1 couples to Gi/o, Gq/11, and G12/13 proteins. The ligand affinity of each LPA receptor is distinct for different LPA species, and multiple studies have reported the distinct structure-activity relationship (SAR) of LPA receptors. The ligand preferences of the LPAR1 were previously comprehensively assessed in Sf9 insect cells and in cells individually transfected with LPA receptor subtypes [17, 18].

Recently, the actions of LPA in the cardiovascular field have received heightened attention [13, 19]. Several studies suggested that LPA has a significant role in the development of vascular wall remodeling, atherosclerosis, and associated pathologies [11, 20, 21]. However, the precise mechanism and their prognostic biomarker value remain unclear. So far little is known about the direct effect of the naturally occurring LPA species on the vascular tone. Under experimental conditions, topically administered 18:1 LPA elicits vasoconstriction in the pial arterioles of newborn piglets, which can be blocked by pertussis toxin (PTX) treatment [22]. It has been also shown that 18:1 LPA enhances the intraluminal pressure-induced myogenic constrictor response in skeletal muscle arterioles. This increase in the myogenic response is not seen after inhibition of LPAR1 & 3 [23].

Our research group has recently reported that the 18:1 LPA induces vasorelaxation via activation of endothelial LPAR1[16]. However, when the endothelial layer is damaged, LPAR1 activation induces cyclooxygenase1 (COX-1) mediated thromboxane A_2 (TXA_2) release, which elicits vasoconstriction [15]. The limitation of our previous study is that this latter pathway was described with the help of a synthetic agonist of the LPAR1-3 (VPC31143), as the 18:1 LPA, which is a full agonist of the LPAR1, evoked only a very weak vasoconstriction. This raises the question, that the complex vascular response to a mixture of different LPA species is not predictable from the SAR of the different LPA molecular species on the LPAR1.

2. Results

2.1. *Vasorelaxation caused by saturated LPA species*

We first examined the activity of the saturated LPAs 14:0, 16:0, 18:0 and 20:0 at 10 μM concentration. We found that only the LPA 14:0 and 16:0 elicited vasorelaxation (Figure 1a). Vasorelaxation diminished with increasing the length of the fatty acid chain. Next, we tested the action of LPA 14:0 and 16:0 in aortae prepared from *Lpar1* KO mice. As shown in Figure 1b, relaxation of the vessels was abolished [p=0.011 for 14:0 LPA; p=0.009 for 16:0 LPA] in vessels prepared from *Lpar1* KO mice, suggesting that vasorelaxation is mediated via LPAR1. In sharp contrast, the 18:0 and 20:0 LPA species failed to elicit vasorelaxation in WT TA segments (Figure 1c)

c).

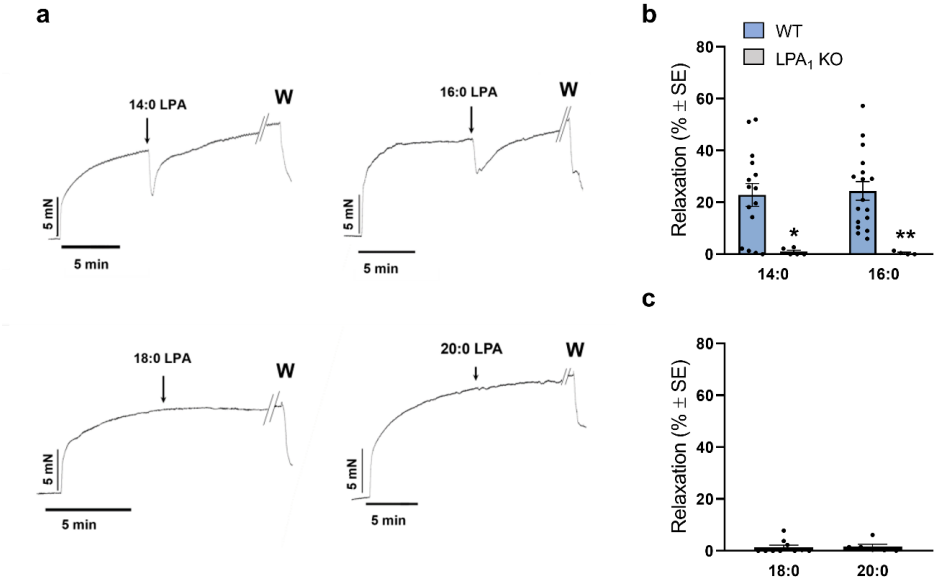

Figure 1. Vasorelaxation evoked by saturated molecular species of LPA. (**a**) Representative recordings of vasorelaxation induced by saturated LPAs in PE precontracted aortic segments prepared from WT and *Lpar1* KO mice. Arrows indicate the administration of 10 μM LPA, W here and subsequent figures stands for the washout. (**b**) Vasorelaxation induced by 10 μM LPA 14:0 and 16:0 in aortic rings prepared from WT and *Lpar1* KO mice [n = 15, 17 WT and 6, 5 LPA1 KO; two-way ANOVA; *p <0.05 vs. WT, **p <0.01 vs. WT]. (**c**) Vasorelaxation induced by 10 μM LPA 18:0 and 20:0 in aortic segments isolated from WT mice (n= 10, 6; unpaired Student's t-test). Bars represent mean ± SEM.

2.2. *Vasoconstrictor activity of saturated LPA species*

In our previous study, vasoconstriction mediated via the LPAR1 elicited by 18:1 LPA was significantly higher in the AA when compared to TA [15]. Therefore, LPA species were applied to the resting tone of endothelium-denuded AA segments to further investigate the SAR of the constrictor response. Similarly to the vasorelaxation, only LPA 14:0 and 16:0 had measurable constrictor effects. We found that the increasing length of the fatty acid chain resulted in a decrease in constrictor activity (Figure 2a; c). The constrictor effect of the 14:0 and 16:0 LPA was largely absent in vessels prepared from *Lpar1* KO animals (p=0.013 for 14:0 LPA; p=0.021 for 16:0 LPA), indicating that the LPAR1 is responsible for the LPA 14:0 and 16:0 induced vasoconstriction (Figure 2b). We were unable to detect vasoconstriction caused by 18:0 and 20:0 LPA.

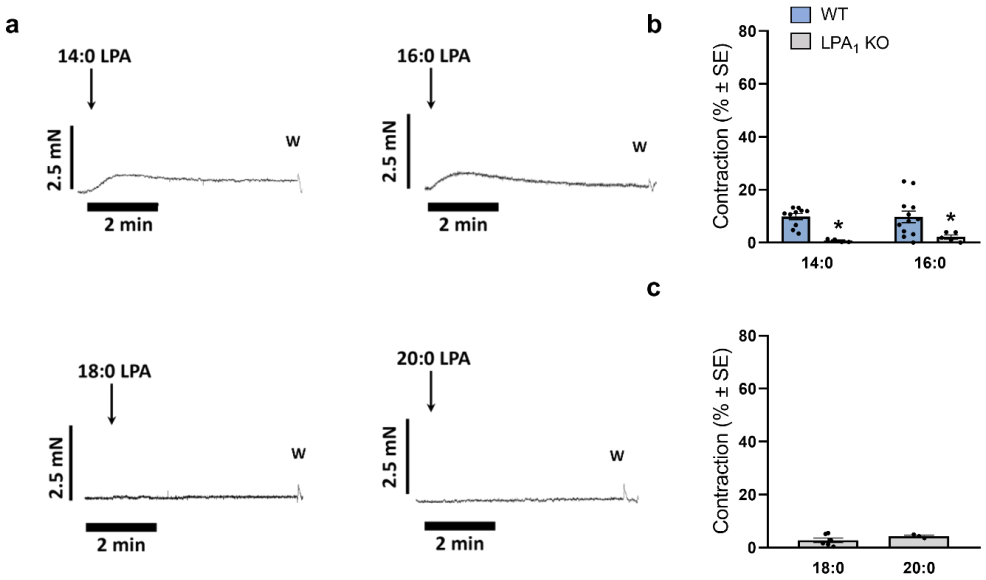

Figure 2. Vasoconstriction evoked by saturated molecular species of LPA. (**a**) Representative recordings of vasoconstriction induced by saturated LPAs in aortic segments prepared from WT mice. Arrows indicate the administration of 10 μM LPA. (**b**) Vasoconstriction induced by 10 μM LPA 14:0 and 16:0 in aortic rings isolated from WT and *Lpar1* KO mice [n = 10, 12 for WT and 4, 5 for LPA_1 KO; two-way ANOVA; *p <0.05 vs. WT]. (**c**) Vasoconstriction induced by 10 μM LPA 18:0 and 20:0 in aortic rings isolated from WT mice (n= 6, 3; unpaired Student's t-test). Bars represent mean ± SEM.

2.3. Vasorelaxation caused by unsaturated LPA species

Next, we evaluated the vasorelaxation elicited by 10 μM concentration of LPA 18:1, 18:2 and 18:3. The mono-unsaturated 18:1 LPA showed a marked vasorelaxation. In contrast, following the relaxation elicited by PU-LPAs, the vascular tone did not return to the precontraction level, but an additional contraction developed (Figure 3a). Comparing the maximal vasorelaxation induced by the C18 LPA species, the relaxation elicited by 18:3 LPA was significantly lower (p=0.002) compared to that of 18:1 LPA (Figure 3d). To get a better insight of the time course of vasorelaxation, we compared the area of the overall vascular response induced by C18 LPA within 5 min after administration of LPA. This analysis revealed that as the degree of unsaturation increased, a shift toward vasoconstriction became apparent (Figure 3e).

To identify the receptor responsible for vasorelaxation, we tested the effect of the unsaturated LPAs in aortic segments isolated from *Lpar1* KO mice (Figure 3b). Unsaturated LPAs failed to induce vasorelaxation in vessels prepared from *Lpar1* KO animals, suggesting that these LPAs elicit vasorelaxation via LPAR1 (Figure 3d). We have reported previously that LPAR1 activation can evoke both vasorelaxation and vasoconstriction [15, 16]. We hypothesized that in aortic segments with an intact endothelium, the response we observe is the superimposition of these two opposing actions on vascular tone. To separately investigate the relaxation response caused by LPA, it was necessary to inhibit the constrictor component of the response. Based on our previous research, where the LPAR1 activation caused COX-mediated vasoconstriction [15], we applied the C18 LPAs to vessels pretreated with 10 μM indomethacin (INDO). Comparison of the peak vasorelaxation induced by these LPAs, only 18:3 LPA induced vasorelaxation was increased significantly (p=0.001) after inhibition of COX (Figure 3d). However, when analyzing the area of the vascular response induced by C18 LPA, the relaxation elicited by both PU-LPA species was increased significantly in the presence of INDO (p<0.0001 for18:2 LPA; p<0.0001 for 18:3 LPA, Figure 3e). In vessels treated with INDO, no significant difference was detected

in the relaxation caused by any C18 LPA species tested (Figure 3c, d, e). This indicated that the cause of the acyl-chain-dependent differences in activity may be related to differences in the constrictor efficacy of the C18 LPAs.

To gain a better understanding into the molecular mechanism underlying the relaxation activity of the C18 LPA species, we measured the Ca^{2+}-signals evoked in endothelial cells. Consistent with the physiological relaxation response, endothelial cells showed a marked rise in intracellular Ca^{2+} when stimulated by 10 μM of the C18 LPA species, which was not influenced by the degree of unsaturation.

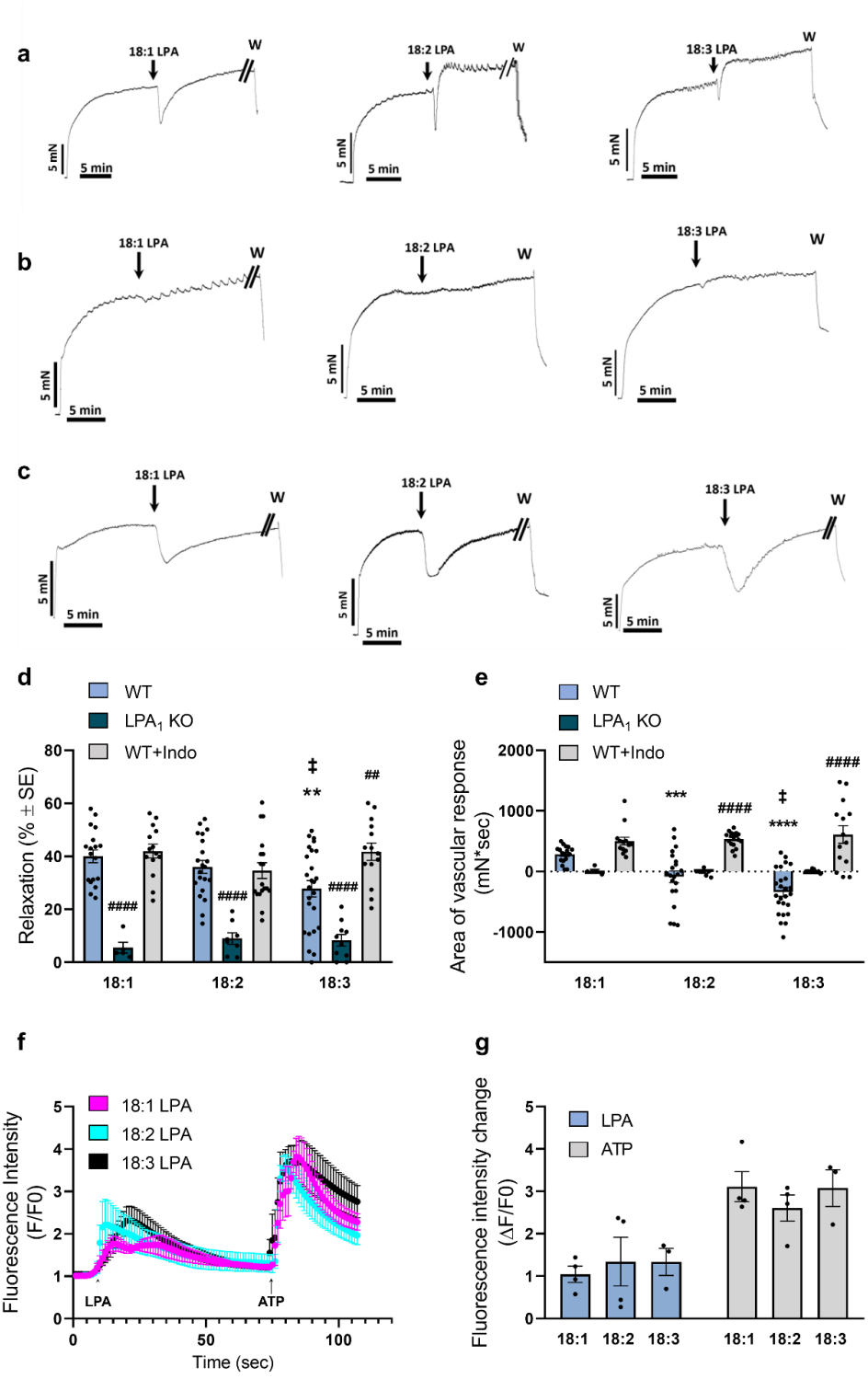

Figure 3. Vasorelaxation induced by unsaturated molecular species of LPA. (**a**) Representative recordings of vasorelaxation elicited by unsaturated LPAs in PE precontracted aortic rings isolated from WT mice. Arrows indicate the administration of 10 μM LPA. (**b**) Representative recordings of vasorelaxation elicited by 10 μM of unsaturated LPA in PE precontracted aortic segments isolated from *Lpar1* knock out (KO) mice. (**c**) Representative recordings of vasorelaxation elicited by 10 μM of unsaturated LPA in PE precontracted aortic segments treated with indomethacin. (**d**) Maximal relaxation activity elicited unsaturated 10 μM 18:1, 18:2 and 18:3 LPAs in aortic rings isolated from WT, *Lpar1* KO mice or in WT aortic segments treated with indomethacin (WT+Indo) [n= 18, 21, 25 (WT); 5, 8, 10 (LPA1 KO); 14, 18, 14 (WT+Indo); two-way ANOVA; **p <0.01 vs. 18:1 WT, ‡p <0.05

vs. 18:2 WT, ##p <0.01 vs. own WT, ####p <0.0001 vs. own WT]. (**e**) Area of vascular response in the first 5 min induced by C18 LPAs (10 μM of each) in aortic rings isolated from WT, *Lpar1* KO mice or in WT aortic segments treated with indomethacin (WT+INDO) (n= 15, 21, 25 in cases of WT; 5, 8, 10 for LPA1 KO;and 9, 18, 14 for WT+Indo; two-way ANOVA; ***p <0.001 vs. 18:1 WT, ****p <0.0001 vs. 18:1 WT, ‡p <0.05 vs. 18:2 WT, ####p <0.0001 vs. own WT]. Positive bars indicate a dominant relaxation, whereas negative bars indicate at constrictor response. (**f**) Average trace of fluorescent intensity in Fluo-4 AM loaded endothelial cells isolated from the aorta of WT mice. Administration of 10 μM of C18 LPAs and 10 μM of ATP are indicated by arrows (n=4, 4, 3). (**g**) Maximal increase in fluorescent intensity evoked by either 10 μM C18 LPA or ATP (n= 4, 4, 3 for LPA; 4, 4, 3 for ATP; one-way ANOVA). Bars represent mean ± SEM.

2.4. *Vasoconstrictor activity of unsaturated LPAs*

Vasoconstriction induced by 10 μM of LPA 18:1, 18:2 and 18:3 (Figure 4a) showed an increasing trend that paralleled the higher number of double bonds. Considering the pathophysiological importance of unsaturated LPA species, we analyzed the dose-response relationship of their vasoconstrictor activity. Analysis of the dose-response relationship showed that 18:1 LPA is a weak constrictor (EC_{50}: 6.67 μM, E_{max}: 27.9%), whereas the efficacy and potency of the constrictor activity of PU-LPA increased significantly (18:1 vs. 18:2 LPA p=0.0012; 18:1 vs. 18:3 LPA p<0.0001; 18:2 vs. 18:3 LPA p<0.0001) [18:2 LPA: EC_{50}: 1.35 μM, E_{max}: 57.8%; 18:3 LPA: EC_{50}: 0.18 μM, E_{max}: 71.6%] (Figure 4b).

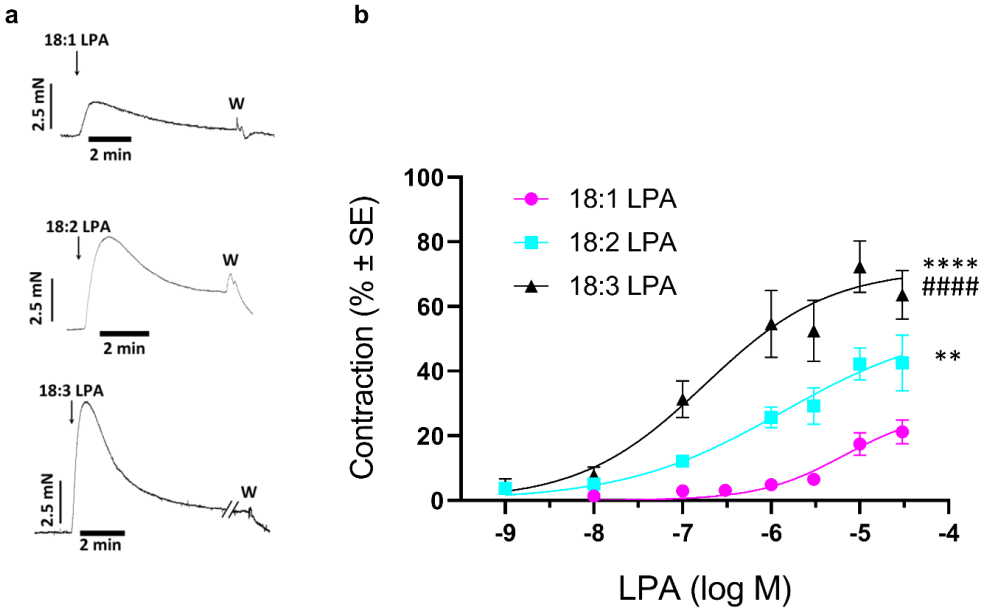

Figure 4. Vasoconstriction evoked by unsaturated molecular species of LPA. (**a**) Representative recordings of vasoconstriction induced by 10 μM of unsaturated LPAs in aortic rings prepared from WT mice. Arrows indicate the administration of 10 μM LPA. (**b**) Dose-response curves for 18:1, 18:2 and 18:3 LPAs induced vasoconstriction in vessels isolated from WT mice (n=3-25; two-way ANOVA; **p <0.01 vs. 18:1 LPA, ****p <0.0001 vs. 18:1 LPA, ####p <0.0001 vs. 18:2 LPA). Bars represent mean ± SEM.

2.5. *Signaling mechanism of vasoconstriction induced by unsaturated LPA*

To establish the role of LPAR1, we examined the constrictor effect of C18 unsaturated LPA species in aortic segments isolated from *Lpar1* KO mice. Vasoconstriction induced by C18 unsaturated LPAs was completely abolished in the vessels prepared from *Lpar1* KO mice, suggesting that the constrictor effect was elicited via LPAR1 (Figure 5a). Similarly, after inhibiting COX with indomethacin, vasoconstriction evoked by unsaturated C18 unsaturated LPA completely disappeared (Figure 5b). As COX activation leads to the release of the potent vasoconstrictor, thromboxane, we measured the TXB_2 released in the effluent of vessels exposed to 10 μM of each C18 unsaturated LPA. PU-LPA 18:2 and 18:3 but not 18:1 LPA increased TXB_2 production in the aortic segments, suggesting the role of prostanoids in the constrictor effect (Figure 5c). Because COX activation is coupled to the G_i protein signaling pathway, next we investigated the constrictor activity of C18 unsaturated LPAs in mice treated intraperitoneally with PTX for 5 days. In aortae isolated from these mice, the average contraction induced by 18:2 and 18:3 LPA was significantly reduced compared with vessels from vehicle treated mice (Figure 5d).

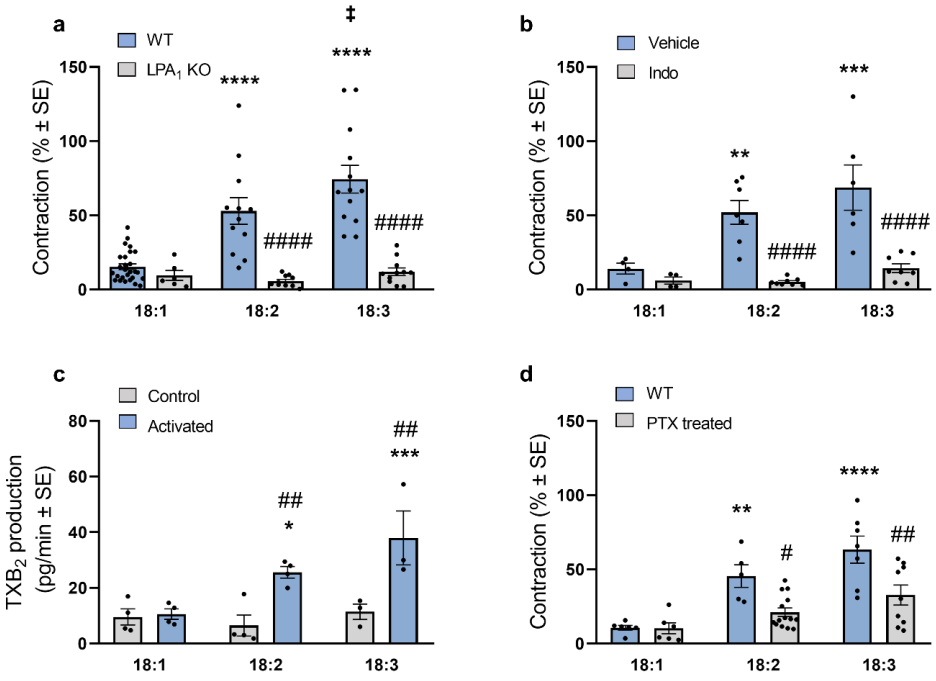

Figure 5. Signaling mechanisms underlying the constrictor activity of unsaturated LPA species. (**a**) Vasoconstriction elicited by LPA species 18:1, 18:2 and 18:3 (10 μM of each) in aortic segments isolated from WT and *Lpar1* KO mice [n = 27, 12, 13 for WT and 6, 10, 11 for LPA1 KO; two-way ANOVA; ****p <0.0001 vs. 18:1 WT, ‡p <0.05 vs. 18:2 WT, ####p <0.0001 vs. own WT]. (**b**) Vasoconstriction induced by C18 LPAs (10 μM of each) in control (Vehicle) and cyclooxygenase inhibited (Indo) vessels isolated from WT mice [n = 4, 7, 6 for vehicle and 4, 8, 8 for Indo; two-way ANOVA; **p <0.01 vs. 18:1 WT, ***p <0.001 vs. 18:1 WT, ####p <0.0001 vs. own WT] (**c**) TXB2 production in aortae before (Control) and after (Activated) treated with 10 μM of C18 LPA (n = 4, 4, 3 for control and 4, 4, 3 for activated vessels; two-way ANOVA; *p <0.05 vs. 18:1 Control, ***p <0.001 vs. 18:1 Control, ##p <0.01 vs. own Control] (**d**) Vasoconstriction elicited by C18 LPAs (10 μM of LPA 18:1, 18:2 and 18:3) in aortic rings isolated from mice treated with vehicle (WT) or pertussis toxin (PTX treated) [n = 6, 5, 7 for WT and 6, 14, 9 for PTX treated; two-way ANOVA; **p <0.01 vs. 18:1 WT, ****p <0.0001 vs. 18:1 WT, #p <0.05 vs. own WT, ##p <0.01 vs. own WT]. Bars represent mean ± SEM.

3.6. Vasoconstriction caused by a combination of LPA species in a ratio that emulates its distribution in plasma

Based on literature data [9], we combined LPA species in a ratio that resembles best to that of ratio of LPA species found in plasma and examined its constrictor effect on endothelium-denuded aortic segments (Figure 6a). As we expected, the combination of LPA species had a minor effect at a concentration of 100 nM similar to that of LPA concentrations found in plasma (Figure 6b, c). However, when the mixture reached a concentration of 10 μM, it induced a marked vasoconstriction (Figure 6b, c). This concentration of LPA mimics what is reached locally in the vicinity of a ruptured plaque.

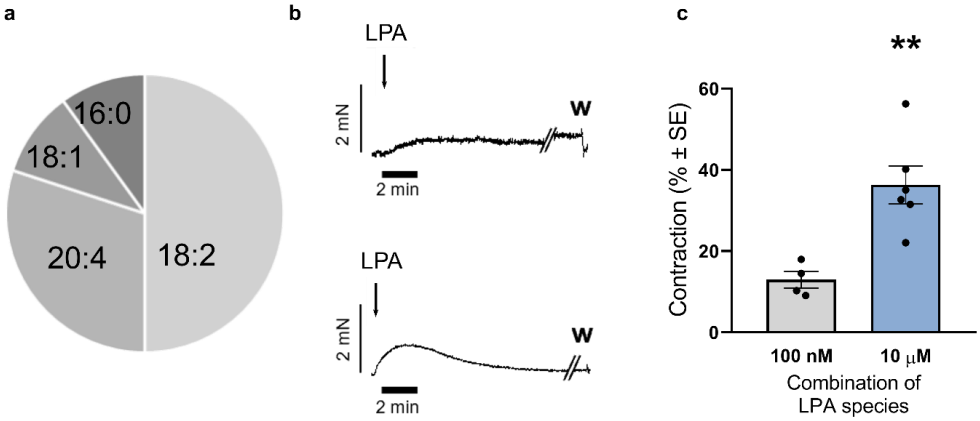

Figure 6. Vasoconstriction evoked by a combination of LPA species with a distribution resembling that of plasma. (**a**) Ratio of the LPA species in the combination. The portion of the pie chart corresponds to the percentage of the specific LPA species. (**b**) Representative recordings of vasoconstriction induced by 100 nm (top) and 10 μM (bottom) of the combination of LPA species in aortic rings prepared from WT mice. Arrows indicate the administration of the combination; W stands for washing out. (**c**) Vasoconstriction induced by 100 nM and 10 μM of the combination of LPA species in aortic rings isolated from WT mice [n = 4 for 100 nM, 6 for 10 μM; unpaired t-test, **p <0.01 vs. 100 nM]. Bars represent mean ± SEM.

3. Discussion

Here we report for the first time that naturally occurring LPA species exhibit markedly different vasoactive effects and different TXA_2-releasing activity. These differences underscore the importance of the difference in elevated plasma levels of specific LPA species in cardiovascular diseases. It is well documented that serum and plasma levels of LPA are increased significantly in certain pathophysiological conditions; however, until now, there was limited experimental evidence about the influence of different naturally occurring LPA species on vascular tone.

Our results indicate that the vasoactive effects triggered by the LPA species examined are solely mediated through the activation of the LPAR1, as the LPA species failed to induce vasorelaxation or vasoconstriction in vessels obtained from *Lpar1* KO mice.

Saturated LPAs with shorter chains have weak relaxing and constrictor effects, but as the chain becomes longer, these effects disappear. The 14:0 LPA was found to have the capability to induce both vasorelaxation and vasoconstriction, which observation aligns with the findings reported by Bandoh et al., who demonstrated that 14:0 LPA can activate signaling pathways through the LPAR1, albeit to a lesser extent [17].

Unsaturated LPAs have higher potency to evoke both vasorelaxation and vasoconstriction via LPAR1. This is agrees with the literature data, as the structure-activity relationship of the LPAR1 in rat hepatoma cells showed the following rank order: 18:2 > 18:3 > 20:4 > 18:1 > 16:0 > 18:0 [18]. Regarding the endothelial effects of the investigated PU-LPA, their vasorelaxant activity decreases with the number of double bonds. The difference in the induced vasorelaxation was even greater when the area of the overall response was analyzed, although this could also be attributed to differences in the rates of elimination. We reported previously that the 18:1 LPA induced vasorelaxation is completely triggered via eNOS activation and intracellular Ca^{2+}-release [16]. However, the difference in the relaxant activity of the C18 LPAs seems not to be due to their ability to induce NO, as they evoke similar vasorelaxation in COX-inhibited aortic segment and a similar Ca^{2+}-signal in endothelial cells, but rather due to a counteracting vasoconstrictor activity elicited only by PU-LPAs.

We found that unsaturated LPA species can elicit vasoconstriction via COX activation and TXA_2 production in the aorta, and both the constrictor response and the released TXA_2 increase in parallel with the increasing number of double bonds up to 3, the highest we have tested. Inhibition of COX diminished the vasoconstriction induced by the C18 LPAs, whereas PTX treatment of the mice significantly inhibited the constrictor response. Intravenously injected LPA species induce transient hypertension in mice. Although unsaturated LPAs evoke hypertension more efficiently than saturated LPAs, which are in agreement with our findings, this hypertensive response is triggered by the LPAR4 and LPAR6 [6]. As relaxation and constriction of the aorta are not major influencing factors of the blood pressure, our findings rather have an impact on determining the thrombogenicity of the vessel wall, as certain LPAs are more prone to elicit NO release, whereas others are capable of considerable TXA_2 release as well. In the case of the monounsaturated 18:1 LPA, aside from its ability to induce vasorelaxation, the released NO may further inhibit thrombo- and atherogenesis by preventing platelet activation, aggregation, adhesion, and by inhibition of smooth muscle cell proliferation and superoxide formation [24]. However, under pathophysiological conditions due to platelet activation, the PU-LPA species, which are the dominant species increased in plasma, the released TXA_2 can overwrite the beneficial effects of NO. This is even more pronounced, when the endothelial layer is damaged, leading to vasoconstriction and increased thrombogenicity vascular wall remodeling [25]. Clearly, further research is needed to clarify, whether these vascular effects are also present in smaller conductance arteries such as the epicardial coronary arteries or carotid artery, as LPA-evoked vasoconstriction may lead to decreased tissue perfusion in the heart and brain, respectively, especially in the case of coexisting endothelial injury. Interestingly, 18:1 LPA can elicit vasorelaxation, but fails to evoke TXA_2 release and produced modest vasoconstriction, though both effects are mediated by the LPAR1. This conflict can be reconciled by the different pharmacological and signaling properties of the LPAR1 in different vascular cell types. Because vasorelaxation is elicited by G_q, whereas vasoconstriction is evoked by G_i signaling pathway, another possible explanation is a signaling bias of the

LPAR1, which has been already reported in the case in human lung fibroblasts [26]. Regarding the vasoactive effects, such signaling bias can be due to differences either in G_q and G_i signaling or the b-arrestin and G protein coupling. Another possible explanation may be the tissue-specific expression of the lipid phosphate phosphatases, which are responsible for the degradation of the LPAs [27], and their different ligand preferences may explain the different constrictor and relaxant effect of the 18:1 LPA. The combined effects of LPA species in a plasma-like composition create that is dominated by polyunsaturated species of LPA elicited a marked vasoconstriction at high yet biologically relevant concentrations of 10 μM.

In conclusion, polyunsaturated C18 LPA species induce marked vasoconstriction via COX-1-derived TXA_2 release, which overrides their endothelial NO-mediated vasorelaxant effect. This phenomenon might become particularly important in cases involving endothelial injury and subsequent platelet activation, where the consequentially released PU-LPAs can contribute to the progression of vasospasm and further platelet activation via initiating thromboxane-mediated signaling. Our results provide an opportunity to advance the understanding of the vasoactive effects of naturally occurring LPA species under both physiological and pathophysiological conditions.

4. Materials and Methods

4.1. Animals

C57Bl/6J mice (range of age 32-38 week) were purchased from Charles River Laboratories (Isaszeg, Hungary), and are referred to as wild type (WT). *Lpar1* knock out (LPAR1 KO) mice were provided by Jerold Chun (Scripps Research Institute, La Jolla, CA, USA) and have been maintained after backcrossing to C57BL/6 since 2008. All animals were housed at constant temperature with a 12/12 h light/dark cycle in a pathogen-free, humidity-controlled environment with ad-libitum access to standard laboratory chow and water. To determine the participation of G_i protein signaling of LPA induced vasoconstriction, mice were injected with PTX intraperitoneally for 5 days at a dose of 30 μg/kg body weight to inhibit the heterotrimeric G_i protein. Control mice were injected with 20% glycerol, which was used to dissolve PTX. Inhibitory effect of PTX was monitored by the disappearance of the acetylcholine (ACh) induced decrease in heart rate (Figure S1).

4.2. Reagents and chemicals

The saturated LPAs (14:0, 16:0, 18:0 LPA) were purchased from Avanti Polar Lipids (Alabaster, AL, USA), whereas the 20:0 LPA and unsaturated LPAs (18:1, 18:2, 18:3, 20:4 LPA) were from Echelon Biosciences Inc. (Salt Lake City, UT, USA). Saturated LPAs were dissolved in methanol, while unsaturated LPAs were dissolved in physiological saline solution and sonicated, immediately before administration. All other reagents were obtained from either Thermo Fisher Scientific (Waltham, MA, USA) or Sigma – Aldrich (Hamburg, Germany).

4.3. Preparation of vessels

Adult male mice were transcardially perfused with 10 ml heparinized (10 IU/ml) Krebs solution (119 mM NaCl, 4.7 mM KCl, 1.2 mM KH2PO4, 2.5 mM CaCl2, 1.2 mM MgSO4·, 20 mM NaHCO3, 0.03 mM EDTA, and 10 mM glucose at 37 °C, pH 7.4) after ether induced deep anaesthesia. Based on our previous studies, to measure vasorelaxation thoracic aortic segments (TA) [16]were used, whereas for the testing vasoconstriction abdominal aortic segments (AA) were isolated [15]. Fat and connective tissue were removed from the vessels under a dissection microscope. The cleaned aorta was cut into 3 mm long segments and placed into the chamber of the wire myograph filled with 6 ml aerated (95% O2–5% CO2), 37°C warm Krebs solution. In the case of measuring vasoconstriction, the endothelial layer was removed by pulling a 3/0 surgical thread through the lumen of the vessel. The absence of the endothelium was confirmed by the disappearance of the ACh evoked vasorelaxation.

4.4. Measurement of the vascular tone

Aortic segments were pulled on stainless steel vessel holders (200 mm in diameter) of the wire myograph (610M Multiwire Myograph System; Danish Myo Technology A/S, Aarhus, Denmark). The segments were incubated for 30 min, while the resting tone of the vessels was adjusted as previously determined [28]. As the first step of our protocol, Krebs solution was replaced by 124 mM K^+ Krebs (made by isomolar replacement of Na to K) solution for 1 min, and the chambers were flushed thoroughly several times with Krebs until the vessels reached their resting tone again. To induce vasoconstriction 10 μM PE was administered to the chamber, followed by 0.1 μM ACh to test the reactivity of the smooth muscle and endothelial cells, respectively. After several rinsing with Krebs solution, vessels were exposed to 124 mM K^+ Krebs for 3 min, which served as a reference contraction throughout this study. After re-establishment of the resting level of the vascular tone by washing the chambers with fresh Krebs solution, a cumulative dose-response relationship of PE (10 nM-10 μM) and ACh (1 nM-10 μM) were examined, respectively. In the case of measuring vasorelaxation, if ACh elicited relaxation was less than 60% of PE induced precontraction, the vessel was excluded from the experiment because of the presumed endothelial damage. When examining vasorelaxation PE-induced vasoconstriction was considered as 100% maximum constriction before LPA was administered. When measuring vasoconstriction, LPA was administered to vessels at their resting tone. In dose-response experiments of the LPA induced vasoconstriction, it was administered in single doses to avoid homologous desensitization of the LPAR1 [29]. At the end of the experiment, to test the robustness of the vessel's response, 124 mM K^+ Krebs solution was applied to the resting tone for 3 min. In some experiments to inhibit COX, vessels were incubated with 10 μM indomethacin for 20 min prior to the administration of LPA. After rinsing with fresh Krebs, 10 μM indomethacin was applied again just before the LPA administration.

4.5. Isolation and of culture of aortic endothelial cells

Complete media for cell cultures was prepared by combining Dulbecco's Modified Eagle Medium (DMEM) with 10 % fetal bovine serum (FBS) and 1% penicillin/streptomycin. The adventitia was removed by gently separating the layers and TAs were cut into 1-

2 mm-long segments. These segments were dissociated enzymatically in digestion solution of 1 ml Hank's Balanced Salt Solution with calcium and magnesium (HBSS++) containing: 1/10 solution of 2.5 mg/ml Liberase TM, 30 U/ml Hyaluronidase and placed into the CO_2 incubator for 1 h. After incubation, 3 mL of complete medium was added to the mix to stop digestion. The cell suspension was centrifuged at 300 x g at room temperature for 5 min, the cell pellet was resuspended in 3 ml of complete medium and centrifuged again under the same conditions. After discarding the supernatant, cells were resuspended in 6 mL pre-warmed complete medium. One ml of the cell suspension was placed into 6-well plates containing gelatin-coated 25 mm diameter coverslips. Cells were grown in a humidified incubator (37 °C, 5% CO_2) for 3 days. Subsequently, the medium was changed every other day.

4.6. Intracellular Ca^{2+} measurement in primary aortic endothelium cells

After 5-8 days, the isolated cells were washed with HBSS++ three times. The cell-loading solution consisted of 2 μM Fluo-4 AM supplemented with Pluronic F-127 (0.02 % v/v) diluted in HBSS++. Cells were incubated in the cell-loading solution at room temperature for 45 min. After incubation, cells were washed with HBSS++ three times. To allow AM-deesterification, cells were incubated for another 30 min in HBSS++ at room temperature. Coverslips were placed into the Attofluor cell chamber (Thermo Fisher Scientific) and imaged using a Nikon, Ti2-E inverted fluorescence microscope under a 20 x/0.75 NA objective. Emission and excitation were recorded at 490 nm and 520 nm, respectively. Images were taken every sec and 10 μM LPA was added after 60 sec of baseline measurement. At the end of the experiment 10 μM of adenosine triphosphate (ATP) was administered to the cells.

4.7. Image analysis

Images were analyzed using the NIS Elements software (Nikon, Japan). After removing the background fluorescence, cells were chosen based on endothelial phenotype which was validated by the previously described immunofluorescence staining (Figure S2). Relative fluorescence intensities were expressed as $\Delta F/F_0$ where F is fluorescence intensity and F_0 is the mean basal fluorescence intensity. Data were plotted over time, where the y axis is F/F_0 and x axis is time in sec.

4.8. Measurement of the TXA_2 release

LPA induced TXA_2 release was measured by TXB_2 enzyme immunoassay kit (Cayman Chemical Co., Ann Arbor, MI, USA) TXA_2 is thermally unstable, it isomerises almost immediately into the stable TXB_2, which is detected by this immunoassay. TAs were isolated as described above. Vessels were cut into 3 mm long segments and were incubated in 37 °C HBSS for 1 h. Segments were exposed to 37 °C warm 200 μl Krebs solution and gently shaken on an orbital shaker for two min. The supernatant was collected, snap frozen in liquid nitrogen, and stored at −80°C. This served as a baseline level of TXA_2 production of the vessels. Subsequently, 200 μl of 10 μM LPA containing Krebs solution was added to the segments for two min, and then the supernatant collected was snap frozen in liquid

nitrogen and stored at −80°C. The immunoassay was performed according to the instructions of the manufacturer and TXB_2 release was expressed as pg/min.

4.9. Statistical evaluation

Biopac MP100 system and AcqKnowledge 3.7.3 software (Biopac System Inc., Goleta, CA, USA) were used to detect changes of the vascular tone. Values of contraction are expressed as a percentage of the maximal contraction elicited 124 mM K^+-Krebs induced, whereas relaxation was normalized to the PE induced precontraction. In the case of the vasorelaxation, the overall area of the vascular response was calculated in the following way: the area under the curve was determined over a 5-min period after LPA administration and subtracted from the area given by the precontraction force extrapolated to 5 min. Therefore, the value of the vascular response is negative if the dominant change in tone is constriction within 5 min following LPA administration. In case of myographic experiments, n indicates the number of vessels, whereas in the case of TXB_2 assay n refers to the number of animals. Statistical analysis was performed with GraphPad Prism software (v.8.01; GraphPad Software Inc., La Jolla, CA, USA). Mean with standard error of the mean (SEM) is presented on the charts. Outliers were filtered using ROUT (robust regression and outlier removal, ROUT coefficient Q = 1%), and normal distributions were checked by Shapiro–Wilk test. Student's unpaired t-test was used to compare two variables, whereas comparing more than two experimental groups, ANOVA was performed followed by Tukey's or Sidak's post hoc test. A p value of <0.05 was considered statistically significant.

5. Conclusions

Although their involvement has been extensively studied in relation to various cardiovascular diseases including atherosclerosis and hypertension, no previous study compared the effect of the naturally occurring LPA species on the vascular tone in situ. Here we show that saturated LPA species have no or minor effect on the vascular tone, whereas unsaturated LPAs have both relaxing and constrictor activity, but the PU-LPA induce enhanced TXA_2 production and lead to pronounced vasoconstriction. Due to the dominance of PU-LPA species after activation of platelets, this can have far-reaching pathophysiological consequences in cardiovascular diseases.

Supplementary Materials: Figure S1: Assessment of the inhibitory effect of PTX in Langendorff-perfused hearts; Figure S2: CD31 expression in primary isolated vascular cell culture.

Author Contributions: É.R, Z.B. and K.V conceptualized and designed the study, J.C. contributed with model; K.V., B.B. and N.K. performed the experiments; K.V., B.B., N.K. and É.R. analyzed data; K.V., Z.B. and É.R. interpreted the results of the experiments; K.E.V. prepared the figures; K.V. and É.R. drafted the manuscript; K.V., B.B., N.K., G.T., Z.B. and É.R edited and revised the manuscript; all authors approved final version of the manuscript.

Funding: This project was supported by the Hungarian National Research, Development, and Innovation Office [K-125174, PD-132851, K-135683, K-139230, NVKP_16-1-2016-0042, EFOP-3.6.3-VEKOP-16-2017-00009] and by the Ministry for Innovation and Technology from the Hungarian NRDI Fund [2020-1.1.6-JÖVŐ-2021-00010; 2020-1.1.6-JÖVŐ-2021-00013; TKP2021-EGA-25].

Institutional Review Board Statement: All animals were treated in accordance with the guideline approved by the National Scientific Ethical Committee on Animal Experimentation (PE/EA/924-7/2021).

Data Availability Statement: The data presented in this study are available on request from the corresponding author (accurately indicate status).

Acknowledgments: We are grateful for Margit Kerék and Ildikó Murányi for expert technical assistance, and we also thank László Hricisák and Ágnes Fülöp (Institute of Translational Medicine, Semmelweis University, Budapest, Hungary) for managing the mouse colonies.

Conflicts of Interest: The authors declare no conflicts of interest.

References

1. Contos, J. J.; Fukushima, N.; Weiner, J. A.; Kaushal, D.; Chun, J., Requirement for the lpA1 lysophosphatidic acid receptor gene in normal suckling behavior. *Proc Natl Acad Sci U S A* **2000,** 97, (24), 13384-9.
2. Inoue, M.; Rashid, M. H.; Fujita, R.; Contos, J. J.; Chun, J.; Ueda, H., Initiation of neuropathic pain requires lysophosphatidic acid receptor signaling. *Nat Med* **2004,** 10, (7), 712-8.
3. Tager, A. M.; LaCamera, P.; Shea, B. S.; Campanella, G. S.; Selman, M.; Zhao, Z.; Polosukhin, V.; Wain, J.; Karimi-Shah, B. A.; Kim, N. D.; Hart, W. K.; Pardo, A.; Blackwell, T. S.; Xu, Y.; Chun, J.; Luster, A. D., The lysophosphatidic acid receptor LPA1 links pulmonary fibrosis to lung injury by mediating fibroblast recruitment and vascular leak. *Nat Med* **2008,** 14, (1), 45-54.
4. Zheng, Y.; Voice, J. K.; Kong, Y.; Goetzl, E. J., Altered expression and functional profile of lysophosphatidic acid receptors in mitogen-activated human blood T lymphocytes. *FASEB J* **2000,** 14, (15), 2387-9.
5. Cheng, Y.; Makarova, N.; Tsukahara, R.; Guo, H.; Shuyu, E.; Farrar, P.; Balazs, L.; Zhang, C.; Tigyi, G., Lysophosphatidic acid-induced arterial wall remodeling: requirement of PPARgamma but not LPA1 or LPA2 GPCR. *Cell Signal* **2009,** 21, (12), 1874-84.
6. Kano, K.; Matsumoto, H.; Inoue, A.; Yukiura, H.; Kanai, M.; Chun, J.; Ishii, S.; Shimizu, T.; Aoki, J., Molecular mechanism of lysophosphatidic acid-induced hypertensive response. *Sci Rep* **2019,** 9, (1), 2662.
7. Williams, J. R.; Khandoga, A. L.; Goyal, P.; Fells, J. I.; Perygin, D. H.; Siess, W.; Parrill, A. L.; Tigyi, G.; Fujiwara, Y., Unique ligand selectivity of the GPR92/LPA5 lysophosphatidate receptor indicates role in human platelet activation. *J Biol Chem* **2009,** 284, (25), 17304-17319.
8. Tigyi, G.; Parrill, A. L., Molecular mechanisms of lysophosphatidic acid action. *Prog Lipid Res* **2003,** 42, (6), 498-526.
9. Kano, K.; Matsumoto, H.; Kono, N.; Kurano, M.; Yatomi, Y.; Aoki, J., Suppressing postcollection lysophosphatidic acid metabolism improves the precision of plasma LPA quantification. *J Lipid Res* **2021,** 62, 100029.
10. Baker, D. L.; Desiderio, D. M.; Miller, D. D.; Tolley, B.; Tigyi, G. J., Direct quantitative analysis of lysophosphatidic acid molecular species by stable isotope dilution electrospray ionization liquid chromatography-mass spectrometry. *Anal Biochem* **2001,** 292, (2), 287-95.
11. Dohi, T.; Miyauchi, K.; Ohkawa, R.; Nakamura, K.; Kishimoto, T.; Miyazaki, T.; Nishino, A.; Nakajima, N.; Yaginuma, K.; Tamura, H.; Kojima, T.; Yokoyama, K.; Kurata, T.; Shimada, K.; Yatomi, Y.; Daida, H., Increased circulating plasma lysophosphatidic acid in patients with acute coronary syndrome. *Clin Chim Acta* **2012,** 413, (1-2), 207-12.
12. Yao, C. S.; Wu, Q. Z.; Xu, H. X.; Liu, F.; Chang, L. G.; Song, L. C.; Gao, L. S.; Meng, X. L., Significant association between lower pulse pressure and increasing levels of a novel type of phospholipid. *Genet Mol Res* **2014,** 13, (2), 2922-30.
13. Kurano, M.; Suzuki, A.; Inoue, A.; Tokuhara, Y.; Kano, K.; Matsumoto, H.; Igarashi, K.; Ohkawa, R.; Nakamura, K.; Dohi, T.; Miyauchi, K.; Daida, H.; Tsukamoto, K.; Ikeda, H.; Aoki, J.; Yatomi, Y., Possible involvement of minor lysophospholipids in the increase in plasma lysophosphatidic acid in acute coronary syndrome. *Arterioscler Thromb Vasc Biol* **2015,** 35, (2), 463-70.
14. Bolen, A. L.; Naren, A. P.; Yarlagadda, S.; Beranova-Giorgianni, S.; Chen, L.; Norman, D.; Baker, D. L.; Rowland, M. M.; Best, M. D.; Sano, T.; Tsukahara, T.; Liliom, K.; Igarashi, Y.; Tigyi, G., The phospholipase A1 activity of lysophospholipase A-I links platelet activation to LPA production during blood coagulation. *J Lipid Res* **2011,** 52, (5), 958-70.

15. Dancs, P. T.; Ruisanchez, E.; Balogh, A.; Panta, C. R.; Miklos, Z.; Nusing, R. M.; Aoki, J.; Chun, J.; Offermanns, S.; Tigyi, G.; Benyo, Z., LPA(1) receptor-mediated thromboxane A(2) release is responsible for lysophosphatidic acid-induced vascular smooth muscle contraction. *FASEB J* **2017,** 31, (4), 1547-1555.
16. Ruisanchez, E.; Dancs, P.; Kerek, M.; Nemeth, T.; Farago, B.; Balogh, A.; Patil, R.; Jennings, B. L.; Liliom, K.; Malik, K. U.; Smrcka, A. V.; Tigyi, G.; Benyo, Z., Lysophosphatidic acid induces vasodilation mediated by LPA1 receptors, phospholipase C, and endothelial nitric oxide synthase. *FASEB J* **2014,** 28, (2), 880-90.
17. Bandoh, K.; Aoki, J.; Taira, A.; Tsujimoto, M.; Arai, H.; Inoue, K., Lysophosphatidic acid (LPA) receptors of the EDG family are differentially activated by LPA species. Structure-activity relationship of cloned LPA receptors. *FEBS Lett* **2000,** 478, (1-2), 159-65.
18. Fujiwara, Y.; Sardar, V.; Tokumura, A.; Baker, D.; Murakami-Murofushi, K.; Parrill, A.; Tigyi, G., Identification of residues responsible for ligand recognition and regioisomeric selectivity of lysophosphatidic acid receptors expressed in mammalian cells. *J Biol Chem* **2005,** 280, (41), 35038-50.
19. Smyth, S. S.; Kraemer, M.; Yang, L.; Van Hoose, P.; Morris, A. J., Roles for lysophosphatidic acid signaling in vascular development and disease. *Biochim Biophys Acta Mol Cell Biol Lipids* **2020,** 1865, (8), 158734.
20. Damirin, A.; Tomura, H.; Komachi, M.; Liu, J. P.; Mogi, C.; Tobo, M.; Wang, J. Q.; Kimura, T.; Kuwabara, A.; Yamazaki, Y.; Ohta, H.; Im, D. S.; Sato, K.; Okajima, F., Role of lipoprotein-associated lysophospholipids in migratory activity of coronary artery smooth muscle cells. *Am J Physiol Heart Circ Physiol* **2007,** 292, (5), H2513-22.
21. Kritikou, E.; van Puijvelde, G. H.; van der Heijden, T.; van Santbrink, P. J.; Swart, M.; Schaftenaar, F. H.; Kroner, M. J.; Kuiper, J.; Bot, I., Inhibition of lysophosphatidic acid receptors 1 and 3 attenuates atherosclerosis development in LDL-receptor deficient mice. *Sci Rep* **2016,** 6, 37585.
22. Tigyi, G.; Hong, L.; Yakubu, M.; Parfenova, H.; Shibata, M.; Leffler, C. W., Lysophosphatidic acid alters cerebrovascular reactivity in piglets. *Am J Physiol* **1995,** 268, (5 Pt 2), H2048-55.
23. Staiculescu, M. C.; Ramirez-Perez, F. I.; Castorena-Gonzalez, J. A.; Hong, Z.; Sun, Z.; Meininger, G. A.; Martinez-Lemus, L. A., Lysophosphatidic acid induces integrin activation in vascular smooth muscle and alters arteriolar myogenic vasoconstriction. *Front Physiol* **2014,** 5, 413.
24. Moncada, S.; Higgs, E. A., Nitric oxide and the vascular endothelium. *Handb Exp Pharmacol* **2006**, (176 Pt 1), 213-54.
25. Nakahata, N., Thromboxane A2: physiology/pathophysiology, cellular signal transduction and pharmacology. *Pharmacol Ther* **2008,** 118, (1), 18-35.
26. Sattikar, A.; Dowling, M. R.; Rosethorne, E. M., Endogenous lysophosphatidic acid (LPA(1)) receptor agonists demonstrate ligand bias between calcium and ERK signalling pathways in human lung fibroblasts. *Br J Pharmacol* **2017,** 174, (3), 227-237.
27. Tang, X.; Benesch, M. G.; Brindley, D. N., Lipid phosphate phosphatases and their roles in mammalian physiology and pathology. *J Lipid Res* **2015,** 56, (11), 2048-60.
28. Horvath, B.; Orsy, P.; Benyo, Z., Endothelial NOS-mediated relaxations of isolated thoracic aorta of the C57BL/6J mouse: a methodological study. *J Cardiovasc Pharmacol* **2005,** 45, (3), 225-31.
29. Alcantara-Hernandez, R.; Hernandez-Mendez, A.; Campos-Martinez, G. A.; Meizoso-Huesca, A.; Garcia-Sainz, J. A., Phosphorylation and Internalization of Lysophosphatidic Acid Receptors LPA1, LPA2, and LPA3. *PLoS One* **2015,** 10, (10), e0140583.

LPA suppresses HLA-DR expression in melanoma: a potential immune escape mechanism involving LPAR1 and DR6 receptor-mediated IL-10 release

Journal:	*Acta Pharmacologica Sinica*
Manuscript ID	Draft
Manuscript Type:	Brief Communication
Date Submitted by the Author:	n/a
Complete List of Authors:	Major, Enikő; Semmelweis University, Institute of Translational Medicine; HUN-REN Hungarian Research Network, HUN-REN-SU Cerebrovascular and Neurocognitive Diseases Research Group Lin, Kuan-Hung; The University of Tennessee Health Science Center, Department of Physiology; Academia Sinica, Institute of Plant and Microbial Biology Lee, Sue Chin; The University of Tennessee Health Science Center, Department of Physiology Káldi, Krisztina; Semmelweis University, Department of Physiology Tigyi, Gábor; The University of Tennessee Health Science Center, Department of Physiology; Semmelweis University, Institute of Translational Medicine Benyó, Zoltán; Semmelweis University, Institute of Translational Medicine; HUN-REN Hungarian Research Network, HUN-REN-SU Cerebrovascular and Neurocognitive Diseases Research Group
Keywords:	melanoma, interleukin-10, HLA-DR, lysophosphatidic acid
Subject Area:	Anticancer Pharmacology

Brief Communication

LPA suppresses HLA-DR expression in melanoma: a potential immune escape mechanism involving LPAR1 and DR6 receptor-mediated IL-10 release

Enikő Major[1,2], Kuan-Hung Lin[3,4], Sue Chin Lee[3], Krisztina Káldi[5], Gábor J. Tigyi[1,3], Zoltán Benyó[1,2]

[1]Institute of Translational Medicine, Semmelweis University, Budapest, Hungary

[2]HUN-REN-SU Cerebrovascular and Neurocognitive Disease Research Group, Hungary

[3]Department of Physiology, University of Tennessee Health Science Centre, Memphis, Tennessee, USA

[4]Institute of Plant and Microbial Biology, Academia Sinica, Taipei, Taiwan

[5]Department of Physiology, Semmelweis University, Budapest, Hungary

Corresponding author:

Zoltán Benyó, MD, PhD, DSc; Institute of Translational Medicine, Semmelweis University, Budapest, Hungary; 37-47 Tűzoltó street, Budapest, H-1094; phone: +3612100306; email: benyo.zoltan@med.semmelweis-univ.hu, ORCID: 0000-0001-6015-0359

Running title: LPA suppresses melanoma HLA-DR via LPAR1-DR6-IL-10 signaling

Abstract

Melanoma is the most aggressive type of skin cancer. While immune checkpoint inhibitors (ICIs) are a promising treatment for metastatic melanoma, approximately 50% of patients do not respond well to them. Recently, elevated expression of human leukocyte antigen-DR (HLA-DR) in tumors has been shown to predict better prognosis and response to ICIs. In the present study, we found that lysophosphatidic acid (LPA), a bioactive lipid mediator, suppresses HLA-DR expression in melanoma cells by upregulating death receptor 6 (DR6) expression. DR6 is inducibly expressed in tumor cells and regulates diverse cellular functions, including cytokine release. Our results reveal that activation of the LPA receptor subtype 1 (LPAR1) via G_i-coupled signaling elicits NF-kB-mediated transcriptional upregulation of DR6 in human melanoma cells. In turn, DR6 upregulates the expression and release of interleukin-10 (IL-10), resulting in diminished HLA-DR expression. These data highlight that the LPAR1-DR6-IL-10 autocrine loop could constitute a novel mechanism used by tumor cells to evade immunosurveillance by decreasing HLA-DR expression.

Keywords: *lysophosphatidic acid; melanoma; death receptor 6; IL-10; LPAR1; HLA-DR*

1. Introduction

The incidence of melanoma is continuously increasing in the Western World and severely impacts patients' life quality and expectancy [1]. A better understanding of the molecular mechanisms of tumor progression and anti-tumor immune response is essential to improve existing therapies and develop new ones for patients with melanoma and other cancers. Lysophosphatidic acid (LPA) is a bioactive lipid mediator produced in large amounts by melanoma and is abundantly present in the tumor microenvironment. LPA regulates a wide range of physiological and pathological cellular functions in almost every cell type via its six G-protein coupled receptors known as LPAR1-6, which can activate several intracellular signaling pathways [2]. In the plasma, LPA is mainly generated from circulating pools of lysophospholipids, primarily from lysophosphatidylcholine, by autotaxin (ATX, encoded by *Enpp2*), an enzyme with lysophospholipase D activity [3]. Interestingly, ATX was first isolated from A2058 human melanoma cells as an "autocrine motility factor" [4]. ATX and LPAR expression is upregulated in several cancer types [5,6] and mediates various aspects of carcinogenesis, including proliferation, survival, migration, angiogenesis, metastasis, and inflammation [7]. In clinical studies, high levels of ATX, which cause elevated LPA levels, are associated with accelerated tumor progression and metastasis formation [8,9]. Furthermore, LPA induces the release of different cytokines and chemokines from tumor cells, which can affect cancer development, metastasis, and tumor immunity [10,11].

Death receptor 6 (DR6, encoded by *Tnfrsf21*) is a recently identified type I transmembrane receptor that belongs to the tumor necrosis factor superfamily. DR6 mRNA is expressed in various organs, including the brain, heart, pancreas, and placenta [12]. Since elevated expression of DR6 has been found to play a pivotal role in numerous human diseases, including Alzheimer's disease, inflammation, and autoimmune disease, it is considered a potential therapeutic target [12]. Similarly, abundant transcript levels of DR6 were observed in several human cancers, indicating a role in tumor biology [13–15]. For example, upregulation of DR6 in lung cancer promotes tumor aggressiveness [20], while low DR6 expression provides a higher overall survival probability in pancreatic adenocarcinoma [16]. Furthermore, Yang et al. revealed that DR6

is required for tumor angiogenesis through the induction of IL-6 via NF-kB-dependent signaling in B16 murine melanoma [17]. DR6 has also been implicated in pro-apoptotic signaling [16]. Interestingly, Dong et al. demonstrated that LPA is able to induce apoptosis via the upregulation of DR6 in HeLa cells [18], although other investigators did not confirm this effect under the same conditions [19].

Interleukin 10 (IL-10) is primarily recognized as an anti-inflammatory cytokine secreted by immune cells. It was later discovered that non-immune cell types, including fibroblasts and keratinocytes, as well as various tumors, such as breast, colon carcinoma, and melanoma, can also produce IL-10 [20]. Although the role of IL-10 in tumor biology is controversial, elevated serum IL-10 levels are reportedly associated with a poor prognosis in melanoma [21–24]. Furthermore, abundant IL-10 expression is accompanied by an increase in other inflammatory mediators and worsens the outcomes of various cancers, indicating that IL-10 can be a key regulator of tumor immunity [25–28].

Tumors can evade immunosurveillance through several mechanisms, including altering the expression of immunologically relevant cell surface molecules and/or creating an immunosuppressive microenvironment through the accumulation of metabolites, cytokines, and chemokines. Although immune checkpoint inhibitors (ICIs) have improved melanoma survival rates, approximately half of patients with metastatic melanoma do not respond well to ICIs [29]. Recently, it was discovered that melanomas with low expression levels of the human leukocyte antigen DR (HLA-DR) respond poorly to immunotherapies [30]. HLA-DR is an MHC class II antigen that is primarily expressed by antigen-presenting cells, but it can also be expressed by other cell types, including tumor cells [31].

Investigating the relation between LPA-LPAR signaling and IL-10-HLA-DR expression represents a previously unexplored topic in melanoma research. As elevated IL-10 levels are frequently associated with poor prognosis in different cancer types, we aimed to examine the potential role of LPA-induced IL-10 release and clarify the underlying signaling mechanisms using human melanoma cells.

2. Materials and methods

2.1 Reagents

18:1 LPA was purchased from Avanti Polar Lipids Inc (Alabaster, AL, USA) and dissolved in 1 mM fatty acid-free bovine serum albumin (Merck KGaA; Darmstadt, Germany). AM095, Ki16425, and pertussis toxin were obtained from Cayman Chemicals (Ann Arbor, MI, USA).

2.2 Cell culture

HEK293T (RRID: CVCL_0063); A2058 (RRID: CVCL_1059), and A375 (RRID: CVCL_0132) human melanoma cells were purchased from the American Type Culture Collection (Rockville, MD, USA). The cell lines were maintained in Dulbecco's Modified Eagle's Medium (DMEM) supplemented with 10% fetal bovine serum (FBS) and 1% Penicillin/Streptomycin and were cultured in a humidified incubator at 37°C and 5% CO_2. Each cell line underwent regular mycoplasma screening, and all experiments were performed using mycoplasma-free cells.

2.3 LPA treatment

In all experiments, cells were serum-starved for 1 hour prior to the administration of LPA. For inhibition of LPAR, the cells were pretreated with AM095 or Ki16425 at 10 μM for 30 minutes prior to treatment with LPA. To investigate G_i protein coupling, the cells were preincubated with 100 ng/mL pertussis toxin (PTX) for 16 hours prior to LPA treatment. Anti-IL-10 neutralizing antibody (JES3-9D7) or IgG1 isotype control (Thermo Fisher Scientific) was administrated at 3.5 μg/mL, 1 hour prior to LPA treatment.

2.4 Luciferase Assay

Genomic DNA was isolated from human keratinocytes using DNeasy Blood&Tissue kit (Qiagen) and used as a template to amplify the predicted hDR6 promoter using a forward and a reverse primer with the sequences 5'-TCCATCGAGCTCTTGGGGGAAGGGTGATTAAA-3' and 5'-

AAAACTCGAGTTCTGCCCAGCGCCGCATCCACC-3', respectively. The amplicon was cloned between the SacI and XhoI restriction sites of the pGL4.10 (Promega, Madison, WI, USA) luciferase expression vector. All constructs were confirmed by sequencing.

HEK293T cells were cultured in 96-well plates. Twenty-four hours after seeding, the cells were co-transfected with the hDR6p-pGL4.10-luc luciferase expression vector and pRL Renilla luciferase control reporter driven by the SV40 promoter (Promega). Plasmid transfection was performed using Lipofectamine3000 (Invitrogen, Karlsruhe, Germany) in OptiMEM (Invitrogen) without supplements, according to the manufacturer's protocol. After 24 hours, cells were kept in a serum-free medium for one hour and treated with 10 μM LPA for the indicated times. Luciferase activities were measured using the Dual-Glo Luciferase Reporter Assay System (Promega) according to the manufacturer's instructions. The relative luciferase activity was calculated by normalizing it to Renilla luciferase activity.

2.5 Gene knockdown

Small interfering RNA (siRNA) targeting DR6 (Catalog ID: L-004450-00-0005) or NF-kB1 (Catalog ID: L-003520-00-0005) mRNA (ON-TARGET*plus* SMARTpool), and non-targeting control (siNC) were purchased from Dharmacon (Lafayette, CO, USA). siRNAs were applied at the time of cell plating in 25 nM final concentration using Lipofectamine RNAiMAX (Invitrogen) according to the manufacturer's instructions. Treatments and measurements were carried out 24 h after transfection.

2.6 Quantitative RT-PCR

RNA was isolated from cells using the NucleoSpin RNA Plus XS kit (Macherey-Nagel GmbH & Co. KG; Düren, Germany). RNA concentration and quality were assessed with Nanodrop (Thermo Fisher Scientific). Up to 1 μg of total RNA was converted to cDNA using the RevertAid First Standard cDNA synthesis kit (Thermo Scientific). RNA expression relative to GAPDH was assessed by quantitative real-time PCR using cDNA corresponding to 40 ng RNA. Reactions were performed with 250 nM of each forward and reverse primers in a final volume of 10 μl of 2XSsoAdvanced Universal SYBR Green Supermix

(BioRad, Hercules, CA). Amplification was performed after one initial denaturation step for 3 min at 98 ºC for 40 cycles at 95 ºC/10 s and 60 ºC/20 s with a CFX Connect™ Real-Time PCR Detection System (BioRad). The fold change of DR6 or IL-10 gene expression normalized to the housekeeping gene (GAPDH) in LPA-treated versus untreated control cells was defined as 2-ΔΔCT. The primer sets used were as follows: GAPDH Fwd: 5'-TCGGAGTCAACGGATTTG-3', Rev: 5'-CAACAATATCCACTTTACCAGAG-3', DR6 Fwd: 5'-GGCATGAACTCAACAGAATC-3', Rev: 5'-GTTGACTACCTGAAGGTTTG-3', IL-10 Fwd: 5'-GCCTTTAATAAGCTCCAAGAG-3', Rev: 5'-ATCTTCATTGTCATGTAGGC-3' (Merck KGaA; Darmstadt, Germany).

2.7 ELISA

Supernatants from melanoma cell cultures were collected after 12 h of 10 μM LPA treatment, and IL-10 concentration was quantified using the Human IL-10 ELISA kit (Abcam) according to the manufacturer's instructions.

2.8 Flow Cytometry

Cells were washed and resuspended in PBS supplemented with 1% bovine serum albumin and stained with a DR6 (7678R, Bioss) or HLA-DR (LN3, Invitrogen) antibody at 4 ºC for 30 min. At least 2 × 10^4 events per sample were counted by using flow cytometry (CytoFLEX, Beckman Coulter Life Sciences; Indianapolis, USA). Data were analyzed with the CytExpertCell software (Beckman Coulter Life Science).

2.9 Statistical Analysis

Statistical analysis was performed using Prism 6 (GraphPad Software Inc.; La Jolla, CA, USA). All data are presented as mean ± SEM obtained from at least three independent experiments. The statistical significances were analyzed using one-way ANOVA and Dunnett's post hoc test. Statistical significance was considered at $p < 0.05$.

3. Results

3.1 Effect of LPA on DR6 receptor expression

First, we aimed to determine the effect of LPA on the expression of the DR6 receptor and found that LPA dose-dependently upregulates the transcript levels of DR6 in HEK293T cells (**Figure 1A**). To investigate the effect of LPA on DR6 promoter activity, luciferase assay was performed in HEK293T cells transfected with a human DR6 promoter construct (**Supplementary Figure S1**). LPA increased the DR6 promoter activity after 30 minutes compared to the vehicle-treated control, and the endogenous expression of DR6 mRNA also increased with a similar time course (**Figure 1B**). Interestingly, whereas the promoter activity declined after 60 min, the mRNA level remained elevated even at 3 h after LPA stimulation.

Our next aim was to identify the receptor mediating the effect of LPA. Of the six LPA GPCRs, LPAR1 and LPAR3 showed the highest expression levels in HEK293T cells (**Supplementary Figure S2**); therefore, we tested if inhibitors specific for either LPAR1/3 (Ki16425) or LPAR1 (AM095) can interfere with the effect of LPA. Both Ki16425 and AM095 were able to inhibit the effect of LPA on DR6 promoter activity (**Figure 1C**) and mRNA levels (**Figure 1D**), suggesting that LPAR1 is the receptor involved in mediating DR6 upregulation.

To explore the potential role of the LPA-DR6 axis in melanoma, we investigated the effect of LPA in inducing DR6 expression in human A375 (**Figure 1E-F**) and A2058 melanoma cells (**Figure G-H**). LPA treatment increased DR6 mRNA and protein levels in both melanoma cell lines. LPA-induced DR6 mRNA transcript level reached a maximum at 1 h (**Figure 1E, G**), whereas the expression of DR6 receptor on the cell surface peaked at 3 h after LPA treatment in both melanoma cell lines (**Figure 1F, H**). Interestingly, in the A375 cell line, LPA induced biphasic expression of the DR6 protein, with a second increase occurring at 12 hours (**Figure 1F**).

3.2 Signaling of LPA-induced DR6 upregulation in human melanoma cells

First, we analyzed the expression levels of different LPA receptors in A2058 and A375 melanoma cells and found that both express predominantly LPAR1 and LPAR3 receptors (**Supplementary Figure S3**). Inhibiting the LPAR1/3 receptors with Ki16425 or selectively LPAR1 using AM095 completely abolished LPA-induced DR6 mRNA expression in both cell lines, supporting a central role of LPAR1 in the process (**Figure 2A** and **D**). To further validate these findings, we used flow cytometry and showed that LPA induced a marked increase in the protein level of DR6, which was inhibited by AM095 in both A375 (**Figure 2B**) and A2058 cells (**Figure 2E**).

To examine the G-protein coupling of LPAR1 to DR6 upregulation, melanoma cells were pretreated with pertussis toxin (PTX), a specific inhibitor of G_i. PTX abrogated the effect of LPA in both melanoma cell lines (**Figure 2A and D**). Using the ALGGEN-PROMO software, we found that the putative promoter sequence of DR6 contains binding sites for the transcription factor (TF) NF-kB1 (**Supplementary Figure S1**). Since LPA is a known activator of NF-kB, we investigated its involvement in LPA-induced DR6 expression. We showed that siRNA silencing of NF-kB1 abrogated the LPA-induced DR6 expression without affecting basal DR6 expression (i.e. in the absence of LPA) (**Figure 2C and F**). Our results indicate that stimulation of the G_i-coupled-LPAR1 by LPA increases DR6 expression via activation of NF-kB1 in both A2058 and A375 melanoma cell lines.

3.3 Effect of LPA on IL-10 production in melanoma

NF-kB plays a central role in the regulation of cytokine networks in malignant cells [32]. Moreover, LPA has been shown to modulate cytokine expression through the activation of NF-kB [33]. As IL-10 has been reported to play a crucial role in melanoma progression , we investigated whether LPA could regulate IL-10 expression. We found that 10 μM LPA increased IL-10 transcript with a similar time course in A2058 and A375 melanoma cells, resulting in maximal mRNA expression at 3h (**Figure 3 A and E**). Using AM095

and PTX, we showed that LPA-induced upregulation of IL-10 is mediated via the LPAR1-G_i pathway (**Figure 3B and F**).

As LPA-induced IL-10 expression appeared to be mediated by the same signaling steps that were previously identified in DR6 upregulation, we hypothesized that DR6 may be involved in the LPA-mediated IL-10 production. Therefore, we evaluated whether silencing the DR6 gene with siRNA interferes with LPA-induced IL-10 mRNA expression. Interestingly, blocking DR6 expression with siRNA reduced IL-10 mRNA levels, indicating that DR6 is responsible for mediating LPA-induced IL-10 expression (**Figures 3C and G**). Moreover, we showed that the LPA-induced secretion of IL-10 in melanoma cells is mediated by LPAR1 and DR6. Specifically, LPA induced a 3- and 5-fold increase in IL-10 secretion in A375 **(Figure 3D)** and A2058 cells **(Figure 3H)**, respectively. These effects were abolished completely by pharmacological inhibition of LPAR1 or silencing of the DR6 gene **(Figure 3D and H)**, providing evidence for the involvement of the LPA-LPAR1-DR6 axis in increasing IL-10 secretion in melanoma.

3.4 Effect of LPA on HLA-DR expression in melanoma

Finally, we investigated whether the LPA-LPAR1-DR6 axis and subsequent IL-10 release affect HLA-DR expression in human melanoma. To do this, we treated A375 or A2058 cells with LPA in the absence and presence of inhibitors of LPAR1 and DR6 or an anti-IL-10 neutralizing monoclonal antibody. Treatment with LPA alone resulted in a marked downregulation of HLA-DR in both A375 **(Figure 4A)** and A2058 melanoma cells **(Figure 4C)**, which was lost after pharmacological inhibition of LPAR1 by AM095 or silencing of the DR6 expression by siDR6. More importantly, the effect of LPA was inhibited by anti-IL-10 neutralizing antibody, which had no influence on HLA-DR expression in the absence of LPA **(Figure 4B and D)**. These results revealed that LPA downregulates HLA-DR expression via activating the LPAR1-DR6-IL-10 pathway in both melanoma cell lines (**Figure 4E**).

4. Discussion

Melanoma is the most aggressive type of skin cancer, which can severely impact life expectancy when the disease has progressed to advanced stages [30]. While ICIs are a promising treatment for metastatic melanoma, approximately 50% of patients do not respond well to them [34,35]. In this study, we used human A375 and A2058 cell lines as representatives of primary and metastatic melanoma models, respectively, to better understand the molecular mechanism by which melanoma can escape the anti-tumor immune response.

Numerous experimental and clinical studies support the role of LPA in tumor development and progression [36]. We hypothesized that LPA-induced IL-10 production contributes to altered expression of HLA antigens, thus modulating the anti-tumor immune response. Under healthy conditions, LPA concentration in the plasma is typically less than 100 nM, but in patients with certain types of malignancies, it is elevated several-fold [37]. Melanoma abundantly expresses autotaxin, the enzyme responsible for the biosynthesis of LPA [38,39]. Autotaxin creates an LPA-rich milieu in the melanoma microenvironment, which can influence tumor progression, metastasis formation, and anti-tumor immunity. The paracrine chemorepulsive effect of autotaxin-derived LPA on tumor-infiltrating lymphocytes and its role in the immune escape of melanoma has been well documented [40]. In the present study, we provide an alternative immune-escape mechanism involving an autocrine effect of LPA on the HLA antigen expression in melanoma cells. Our results indicate that LPA downregulates HLA-DR, the expression of which has recently been reported to strongly correlate with the therapeutic efficacy of ICIs [30]. This effect of LPA involves LPAR1-, G_i-protein- and NF-kB-mediated upregulation of DR6 and consequent IL-10 release.

Although upregulated DR6 expression has been reported in several tumor types, including melanoma [13,14], where a clinical study reported its association with chemotherapy resistance [47], the exact role of DR6 in tumor biology remained obscure. We show that LPA regulates DR6 expression by acting on LPAR1. Furthermore, our results with PTX support the role of G_i-protein in mediating the effect. The role of LPAR1

in LPA-induced cancer invasion and oncogenesis is well established [42]. In many primary tumors, elevated LPAR1 expression correlates with increased proliferation and poor prognosis [42,43]. Moreover, LPAR1 was identified as a crucial regulator of melanoma invasion, metastasis, and therapy resistance [44]. However, the present study is the first report on the role of LPA and LPAR1 in modulating HLA-DR expression.

Our findings that LPA increased DR6 promoter activity and mRNA expression after 30 min indicate that it acts as an immediate-early gene that responds to LPA. We examined the promoter sequence of DR6 and found that it contains binding sites for NF-kB1 (p50). Our results showed that silencing NF-kB1 inhibited LPA-induced DR6 expression, confirming its role in mediating DR6 upregulation. NF-kB1 is known as an essential regulator of cell survival in cancer [45]. It has been reported that p50 and p65, members of the NF-kB family, are overexpressed in melanoma cells compared to non-transformed melanocytes, supporting their contribution to cancer development [46].

Although LPA is a known mediator of cytokine release [47], its role in regulating IL-10 expression by tumor cells has not been described previously. In LPS-stimulated human dendritic cells and macrophages, LPA has been reported to increase IL-10 release with subsequent inhibition of TNF-α production [48]. IL-10 is an important immunosuppressive cytokine that is frequently upregulated in the tumor microenvironment [49,50]. In clinical studies, IL-10 expression and production were shown to correlate with melanoma progression [27]. Sato et al. reported that transformed melanocytes are a major source of IL-10 production in melanoma metastases [50]. Our study is the first to report on LPA-induced IL-10 production by tumor cells and identifies LPAR1-dependent upregulation of DR6 receptors in mediating this effect.

IL-10 can inhibit essential steps in immune detection by decreasing the cell surface expression of HLA class I and II antigens as well as the intercellular adhesion molecule-1 (ICAM-1) in melanoma cells [51]. The efficacy of immunotherapy depends on the identification of the cell surface antigens by T cells [30]. In

cancerous diseases, low expression of HLA-DR, a MHC-II isotype antigen, is often associated with poor survival [52]. Although HLA-DR expression alone does not appear to determine the prognosis, it strongly influences the therapeutic efficacy of ICIs in melanoma [30]. Recently, numerous retrospective clinical studies proved that tumor cell HLA-DR positivity is associated with a higher response rate for ICI immunotherapy in patients with advanced melanoma [53,54]. In response to ICI, significantly better progression-free and overall survival were observed in the HLA-DR positive tumors compared to HLA-DR negative ones (tumors with less than 5% HLA-DR+ melanoma cells) [30]. Our results established that LPA significantly downregulates the HLA-DR expression in human melanoma cells, which is a novel mechanism of LPA-induced immune escape. Supporting our findings, Konen et al. demonstrated that ATX and LPA are upregulated in anti-PD-1 resistant non-small cell lung cancer and negatively correlated with the number of infiltrating CD8+ T cells [55], indicating that increased LPA levels negatively affect the response to ICI. The present study reveals a connection between the elevated LPA concentration and IL-10 production, which in turn diminishes the HLA-DR expression in melanoma. Furthermore, our results demonstrated that the knockdown of DR6 by siRNA abolished the effect of LPA on IL-10 expression and production, reinforcing the central role of DR6 in LPA-induced cytokine release by tumor cells.

In summary, the present study demonstrates that LPA increases DR6 expression in a G_i-coupled LPAR1- and NF-kB-dependent manner. Moreover, LPA is a potent regulator of IL-10 gene transcription and protein release via DR6, resulting in decreased HLA-DR expression in melanoma cells (**Figure 5**). Because IL-10 plays an important role in the immune escape of tumors and neutralizing IL-10 has been proposed as a novel anti-tumor therapy [56,57], downregulation of HLA-DR through LPA-induced IL-10 production might be an important pathway in the progression, metastasis, and immune escape of melanoma.

Acknowledgments

Figure 5 and Supplementary Figure S1 were created with BioRender.com.

Funding

This study was supported by NKFIH K-125174, K-132393, K-135683 and K-139230, as well as by 2020-1.1.6-JÖVŐ-2021-00010, TKP2021-EGA-25 and EFOP-3.6.3-VEKOP-16-2017-00009 grants, by the Talentum Foundation by Gedeon Richter Plc, NCI grant CA092660, the Harriet Van Vleet Endowment and HUN-REN Hungarian Research Network.

Conflict of interest

The authors declare that they have no known competing financial interests or personal relationships that could have appeared to influence the work reported in this paper.

Author contributions

EM designed and developed the study under the supervision of ZB, GT, KK, SCL, KHL and performed the experiments. Funding acquisition and resources were provided by GT, KK, and ZB. All authors reviewed and approved the manuscript.

Data availability

The datasets used during the present study are available from the corresponding author upon a reasonable request.

Supplementary information is available at the website of Acta Pharmacologica Sinica.

References

1 Siegel RL, Miller KD, Fuchs HE, Jemal A. Cancer Statistics, 2021. *CA Cancer J Clin*. 2021;**71**(1):7–33.

2 Tigyi G. Aiming drug discovery at lysophosphatidic acid targets. *Br J Pharmacol*. 2010;**161**(2):241–270.

3 Benesch MGK, Ko YM, McMullen TPW, Brindley DN. Autotaxin in the crosshairs: Taking aim at cancer and other inflammatory conditions. *FEBS Lett*. 2014;**588**(16):2712–2727.

4 Stracke ML, Krutzsch HC, Unsworth EJ, Arestad A, Cioce V, Schiffmann E, et al. Identification, purification, and partial sequence analysis of autotaxin, a novel motility-stimulating protein. *Journal of Biological Chemistry*. 1992;**267**(4):2524–2529.

5 Yu S, Murph MM, Lu Y, Liu S, Hall HS, Liu J, et al. Lysophosphatidic acid receptors determine tumorigenicity and aggressiveness of ovarian cancer cells. *J Natl Cancer Inst*. 2008;**100**(22):1630–1642.

6 Li TT, Alemayehu M, Aziziyeh AI, Pape C, Pampillo M, Postovit LM, et al. Beta-arrestin/Ral signaling regulates lysophosphatidic acid-mediated migration and invasion of human breast tumor cells. *Mol Cancer Res*. 2009;**7**(7):1064–1077.

7 Gotoh M, Fujiwara Y, Yue J, Liu J, Lee SC, Fells J, et al. Controlling cancer through the autotaxin-lysophosphatidic acid receptor axis. *Biochem Soc Trans*. 2012;**40**(1):31–36.

8 Li Y-Y, Zhang W-C, Zhang J-L, Zheng C-J, Zhu H, Yu H-M, et al. Plasma levels of lysophosphatidic acid in ovarian cancer versus controls: a meta-analysis. *Lipids Health Dis*. 2015;**14**(1):72.

9 Chen J, Li H, Xu W, Guo X. Evaluation of serum ATX and LPA as potential diagnostic biomarkers in patients with pancreatic cancer. *BMC Gastroenterol*. 2021;**21**(1):1–10.

10 Lee SC, Dacheux MA, Norman DD, Balázs L, Torres RM, Augelli-Szafran CE, et al. Regulation of Tumor Immunity by Lysophosphatidic Acid. *Cancers 2020, Vol 12, Page 1202*. 2020;**12**(5):1202.

11 Lee D, Suh DS, Lee SC, Tigyi GJ, Kim JH. Role of Autotaxin in Cancer Stem Cells. *Cancer Metastasis Rev*. 2018;**37**(2–3):509.

12 Ren X, Lin Z, Yuan W. A Structural and Functional Perspective of Death Receptor 6. *Front Pharmacol*. 2022;**13**:776.

13 Stegmann S, Werner JM, Kuhl S, Röhn G, Krischek B, Stavrinou P, et al. Death Receptor 6 (DR6) Is Overexpressed in Astrocytomas. *Anticancer Res*. 2019;**39**(5):2299–2306.

14 McNeal S, Bitterman P, Bahr JM, Edassery SL, Abramowicz JS, Basu S, et al. Association of Immunosuppression with DR6 Expression during the Development and Progression of Spontaneous Ovarian Cancer in Laying Hen Model. *J Immunol Res*. 2016;**2016**.

15 Kasof GM, Lu JJ, Liu D, Speer B, Mongan KN, Gomes BC, et al. Tumor necrosis factor-alpha induces the expression of DR6, a member of the TNF receptor family, through activation of NF-kappaB. *Oncogene*. 2001;**20**(55):7965–7975.

16 Xu H, Yin L, Xu Q, Xiang J, Xu R. N6-methyladenosine methylation modification patterns reveal immune profiling in pancreatic adenocarcinoma. *Cancer Cell Int*. 2022;**22**(1):1–17.

17 Yang X, Shi B, Li L, Xu Z, Ge Y, Shi J, et al. Death receptor 6 (DR6) is required for mouse b16 tumor angiogenesis via the NF-κB, P38 MAPK and STAT3 pathways. *Oncogenesis*. 2016;**5**(3).

18 Dong Y, Wu Y, Cui MZ, Xu X. Lysophosphatidic Acid Triggers Apoptosis in HeLa Cells through the Upregulation of Tumor Necrosis Factor Receptor Superfamily Member 21. *Mediators Inflamm*. 2017;**2017**.

19 Wang X, Wang H, Mou X, Xu Y, Han W, Huang A, et al. Lysophosphatidic acid protects cervical cancer HeLa cells from apoptosis induced by doxorubicin hydrochloride. *Oncol Lett*. 2022;**24**(2):1–8.

20 Carlini V, Noonan DM, Abdalalem E, Goletti D, Sansone C, Calabrone L, et al. The multifaceted nature of IL-10: regulation, role in immunological homeostasis and its relevance to cancer, COVID-19 and post-COVID conditions. *Front Immunol*. 2023;**14**:1161067.

21 Dummer W, Becker JC, Schwaaf A, Leverkus M, Moll T, Bröcker EB. Elevated serum levels of interleukin-10 in patients with metastatic malignant melanoma. *Melanoma Res*. 1995;**5**(1):67–68.

22 Nemunaitis J, Fong T, Shabe P, Martineau D, Ando D. Comparison of serum interleukin-10 (IL-10) levels between normal volunteers and patients with advanced melanoma. *Cancer Invest*. 2001;**19**(3):239–247.

23 Zhao H, Yang J, Yu Z, Shen H, Huang X, Zhang M, et al. Synthetic analysis of associations between IL-10 polymorphisms and skin cancer risk. *Oncotarget*. 2017;**9**(6):6728–6736.

24 Lippitz BE. Cytokine patterns in patients with cancer: A systematic review. *Lancet Oncol*. 2013;**14**(6):e218–e228.

25 Zhao S, Wu D, Wu P, Wang Z, Huang J, Gao JX. Serum IL-10 Predicts Worse Outcome in Cancer Patients: A Meta-Analysis. *PLoS One*. 2015;**10**(10).

26 Krüger-Krasagakes S, Krasagakis K, Garbe C, Schmitt E, Hüls C, Blankenstein T, et al. Expression of interleukin 10 in human melanoma. *British Journal of Cancer 1994 70:6*. 1994;**70**(6):1182–1185.

27 Itakura E, Huang RR, Wen DR, Paul E, Wünsch PH, Cochran AJ. IL-10 expression by primary tumor cells correlates with melanoma progression from radial to vertical growth phase and development of metastatic competence. *Modern Pathology*. 2011;**24**(6):801–809.

28 Hsu T-I, Wang Y-C, Hung C-Y, Yu C-H, Su W-C, Chang W-C, et al. Positive feedback regulation between IL10 and EGFR promotes lung cancer formation. *Oncotarget*. 2016;**7**(15):20840–20854.

29 Kim SK, Cho SW. The Evasion Mechanisms of Cancer Immunity and Drug Intervention in the Tumor Microenvironment. *Front Pharmacol*. 2022;**13**.

30 Amrane K, Le Meur C, Besse B, Hemon P, Le Noac'h P, Pradier O, et al. HLA-DR expression in melanoma: from misleading therapeutic target to potential immunotherapy biomarker. *Front Immunol*. 2024;**14**:1285895.

31 Axelrod ML, Cook RS, Johnson DB, Balko JM. Biological consequences of MHC-II expression by tumor cells in cancer. *Clinical Cancer Research*. 2019;**25**(8):2392–2402.

32 Taniguchi K, Karin M. NF-κB, inflammation, immunity and cancer: coming of age. *Nature Reviews Immunology 2018 18:5*. 2018;**18**(5):309–324.

33 Sun W, Yang J. Molecular basis of lysophosphatidic acid-induced NF-κB activation. *Cell Signal*. 2010;**22**(12):1799–1803.

34 Michielin O, Atkins MB, Koon HB, Dummer R, Ascierto PA. Evolving impact of long-term survival results on metastatic melanoma treatment. *J Immunother Cancer*. 2020;**8**(2).

35 Olbryt M, Rajczykowski M, Widłak W. Biological Factors behind Melanoma Response to Immune Checkpoint Inhibitors. *Int J Mol Sci*. 2020;**21**(11):E4071–E4071.

36 Aiello S, Casiraghi F. Lysophosphatidic Acid: Promoter of Cancer Progression and of Tumor Microenvironment Development. A Promising Target for Anticancer Therapies? *Cells 2021, Vol 10, Page 1390*. 2021;**10**(6):1390.

37 Sedláková I, Vávrová J, Tošner J, Hanousek L. Lysophosphatidic acid (LPA) - A perspective marker in ovarian cancer. *Tumor Biology*. 2011;**32**(2):311–316.

38 Jankowski M. Autotaxin: Its role in biology of melanoma cells and as a pharmacological target. *Enzyme Res*. 2011;**2011**(1).

39 Tigyi G, Dacheux MA, Lin KH, Yue J, Norman D, Benyó Z, et al. Anti-cancer strategies targeting the autotaxin-lysophosphatidic acid receptor axis: is there a path forward? *Cancer and Metastasis Reviews*. 2021;**40**(1):3–5.

40 Matas-Rico E, Frijlink E, van der Haar Àvila I, Menegakis A, van Zon M, Morris AJ, et al. Autotaxin impedes anti-tumor immunity by suppressing chemotaxis and tumor infiltration of CD8+ T cells. *Cell Rep*. 2021;**37**(7).

41 Chen R, Niu L, Wu L, He Y, Liu G, Hong K. Identification of an endoplasmic reticulum stress-associated gene signature to predict the immune status and prognosis of cutaneous melanoma. *Medicine (United States)*. 2022;**101**(36):E30280.

42 Zhao P fei, Wu S, Li Y, Bao G, Pei J yuan, Wang Y wu, et al. LPA receptor1 antagonists as anticancer agents suppress human lung tumours. *Eur J Pharmacol*. 2020;**868**.

43 Cui R, Cao G, Bai H, Zhang Z. LPAR1 regulates the development of intratumoral heterogeneity in ovarian serous cystadenocarcinoma by activating the PI3K/AKT signaling pathway. *Cancer Cell Int*. 2019;**19**(1).

44 Liu J, Rebecca VW, Kossenkov A V., Connelly T, Liu Q, Gutierrez A, et al. Neural Crest-Like Stem Cell Transcriptome Analysis Identifies LPAR1 in Melanoma Progression and Therapy Resistance. *Cancer Res*. 2021;**81**(20):5230–5241.

45 Verzella D, Pescatore A, Capece D, Vecchiotti D, Ursini MV, Franzoso G, et al. Life, death, and autophagy in cancer: NF-κB turns up everywhere. *Cell Death & Disease 2020 11:3*. 2020;**11**(3):1–14.

46 McNulty SE, Del Rosario R, Cen D, Meyskens FL, Yang S. Comparative Expression of NFκB Proteins in Melanocytes of Normal Skin vs. Benign Intradermal Naevus and Human Metastatic Melanoma Biopsies. *Pigment Cell Res*. 2004;**17**(2):173–180.

47 Leblanc R, Houssin A, Peyruchaud O. Platelets, autotaxin and lysophosphatidic acid signalling: win-win factors for cancer metastasis. *Br J Pharmacol*. 2018;**175**(15):3100–3110.

48 Ciesielska A, Hromada-Judycka A, Ziemlińska E, Kwiatkowska K. Lysophosphatidic acid up-regulates IL-10 production to inhibit TNF-α synthesis in Mϕs stimulated with LPS. *J Leukoc Biol*. 2019;**106**(6):1285–1301.

49 Mahipal A, Terai M, Berd D, Chervoneva I, Patel K, Mastrangelo MJ, et al. Tumor-derived interleukin-10 as a prognostic factor in stage III patients undergoing adjuvant treatment with an autologous melanoma cell vaccine. *Cancer Immunol Immunother*. 2011;**60**(7):1039–1045.

50 Sato T, McCue P, Masuoka K, Salwen S, Lattime EC, Mastrangelo MJ, et al. Interleukin 10 production by human melanoma. *Clinical Cancer Research*. 1996;**2**(8):1383–1390.

51 Yun YUE F, Dummer R, Geertsen R, Hofbauer G, Laine E, Manolio S, et al. INTERLEUKIN-10 IS A GROWTH FACTOR FOR HUMAN MELANOMA CELLS AND DOWN-REGULATES HLA CLASS-I, HLA CLASS-II AND ICAM-1 MOLECULES. *J Cancer*. 1997;**71**:630–637.

52 Dunne MR, Michielsen AJ, O'Sullivan KE, Cathcart MC, Feighery R, Doyle B, et al. HLA-DR expression in tumor epithelium is an independent prognostic indicator in esophageal adenocarcinoma patients. *Cancer Immunology, Immunotherapy*. 2017;**66**(7):841.

53 Johnson DB, Estrada M V., Salgado R, Sanchez V, Doxie DB, Opalenik SR, et al. Melanoma-specific MHC-II expression represents a tumour-autonomous phenotype and predicts response to anti-PD-1/PD-L1 therapy. *Nat Commun*. 2016;**7**.

54 Toki MI, Merritt CR, Wong PF, Smithy JW, Kluger HM, Syrigos KN, et al. High-plex predictive marker discovery for melanoma immunotherapy-treated patients using digital spatial profiling. *Clinical Cancer Research*. 2019;**25**(18):5503–5512.

55 Konen JM, Leticia Rodriguez B, Wu H, Fradette JJ, Gibson L, Diao L, et al. Autotaxin suppresses cytotoxic T cells via LPAR5 to promote anti–PD-1 resistance in non–small cell lung cancer. *J Clin Invest*. 2023;**133**(17).

56 Mirlekar B. Tumor promoting roles of IL-10, TGF-β, IL-4, and IL-35: Its implications in cancer immunotherapy. *SAGE Open Med*. 2022;**10**.

57 Sullivan KM, Jiang X, Guha P, Lausted C, Carter JA, Hsu C, et al. Blockade of interleukin 10 potentiates antitumour immune function in human colorectal cancer liver metastases. *Gut*. 2023;**72**(2):325–337.

Figure 1. Upregulation of DR6 induced by LPA. A) HEK293T cells were treated with the indicated concentrations of LPA for 30 min and DR6 expression was measured using qPCR. B) HEK293T cells transfected with the DR6 promoter construct were treated with 10 μM LPA for the indicated times and luciferase activity was measured (red line). Relative expression of the DR6 transcript was analyzed by qPCR

(green line). C) HEK293T cells transfected with DR6 promoter construct were treated with 10 μM LPA for 30 minutes. Where indicated, cells were pretreated with either 10 μM LPAR1/3 inhibitor Ki16425 or 10 μM LPAR1 inhibitor AM095. D) The inhibition with Ki16425 or AM095 on the LPA-induced upregulation of DR6 was confirmed by qPCR. E-H) Melanoma cells were treated with 10 μM LPA. Time-dependent induction of DR6 expression was followed by qPCR (E, G) and flow cytometry (F, H). **P*<0.05, ***P*<0.01, ****P*<0.001, *****P*<0.0001 vs. CONT, #*P*<0.0004 vs LPA alone, One-way ANOVA, Dunnett's posthoc test

Figure 2. Activation of the G_i-coupled LPAR1 of melanoma cells increases DR6 expression in an NF-kB-dependent manner. Human melanoma cells were treated with 10 μM LPA for 1 h in the presence of 10 μM Ki16425 or 10 μM AM095. The pretreatment with PTX (100 ng/mL) was administered at least 16 h prior to the LPA treatment. Gene expression was evaluated by qPCR (A, D). B) The inhibitory effect of AM095 on DR6 protein expression was analyzed by flow cytometry (B, E). NF-kB1 was transiently silenced by siRNA to assess its role in the induction of DR6 by LPA (C, F). **P*<0.05, ***P*<0.01, ****P*<0.001, *****P*<0.0001 vs. CONT; #*P*<0.0008 vs. LPA alone, One-way ANOVA, Dunnett's posthoc test

Figure 3. Regulation of LPA-driven IL-10 expression in human melanoma cells. Melanoma cells were treated with 10 μM LPA. Time-dependent induction of IL-10 expression was examined by qPCR (A, E). AM095 and PTX were used to examine the G_i-coupled LPAR1 signaling (B, F). When indicated, NF-kB1 and DR6 were silenced by siRNA (C, G). D-H) siNC or siDR6-transfected A375 and A2058 melanoma cells were treated with 10 μM LPA or its vehicle for 12 h in the presence or absence of AM095. The level of IL-10 was determined in the supernatants of the cells. **P*<0.05, ***P*<0.01, ****P*<0.001, *****P*<0.0001vs CONT, #*P*<0.0008 vs. LPA alone, One-way ANOVA, Dunnett's posthoc test

Figure 4. LPA-induced downregulation of HLA-DR in human melanoma. A375 and A2058 cells were treated with 10 μM LPA for 22h. HLA-DR expression was measured by flow cytometry. The signaling pathway was examined using AM095 or siDR6 (A, C). IL-10 was neutralized by an anti-IL10 monoclonal

antibody, and IgG1 kappa was used as isotype control (B, D). ***P*<0.008, *****P*<0.0001 vs. CONT, #*P*<0.05 vs. LPA One-way ANOVA, Dunnett's posthoc test

Figure 5. Signaling pathways of LPA-induced downregulation of HLA-DR in melanoma. LPA, via its G_i-coupled LPAR1 receptor, activates NF-kB-mediated DR6 expression, which in turn activates the transcription and secretion of IL-10. LPA-mediated IL-10 release leads to the downregulation of HLA-DR antigen in human melanoma cells. (Created with BioRender.com).

Supporting information

Supplementary Figure S1. The putative promoter region of human DR6 was identified using the Berkley NNPP program.

Supplementary Figure S2. LPAR mRNA profile of HEK293T cells.

Supplementary Figure S3. LPAR mRNA profile of A375 and A2058 cells.

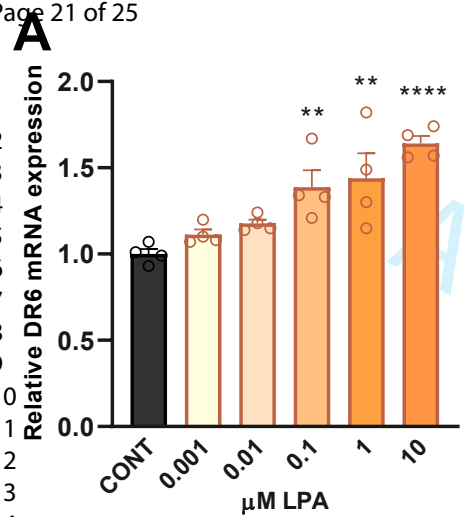

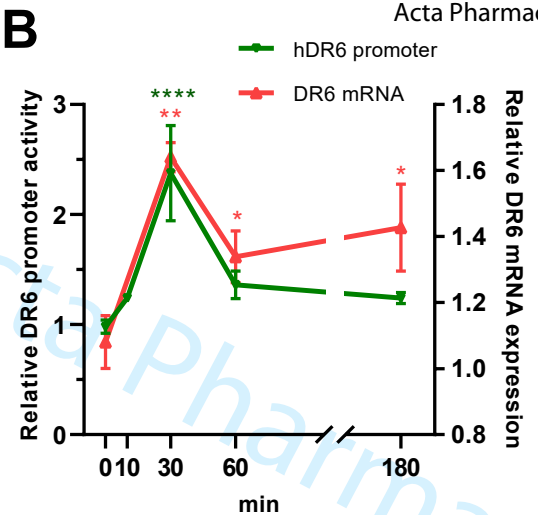

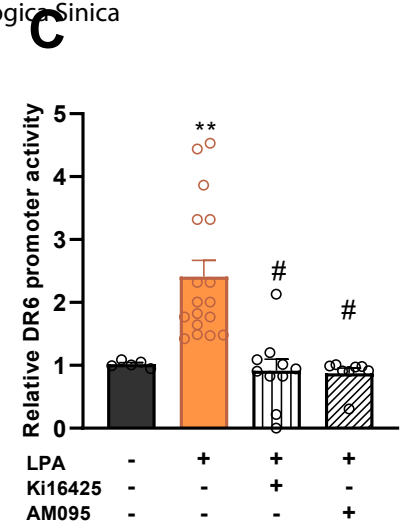

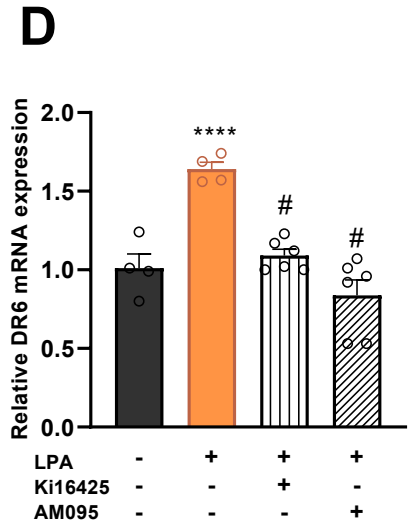

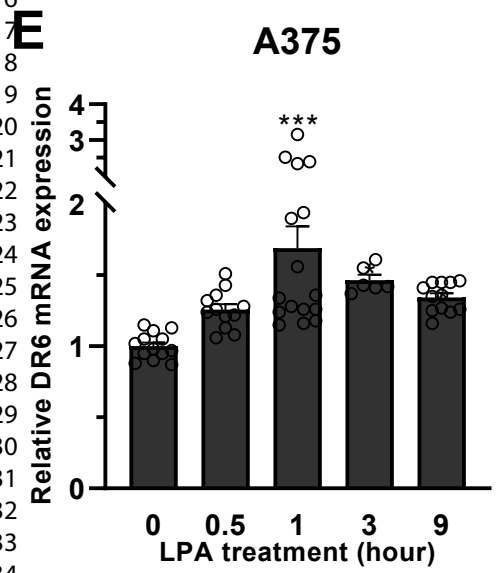

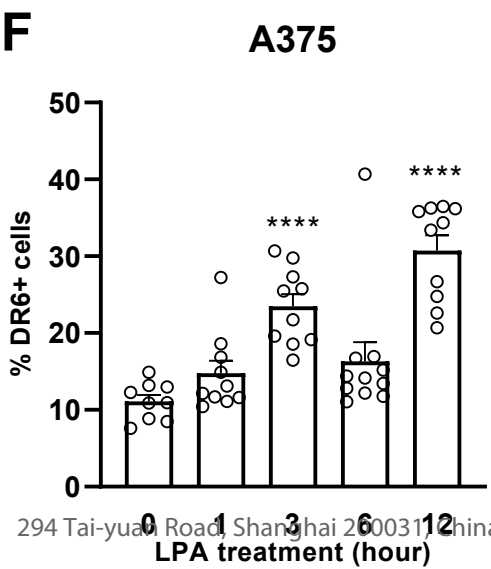

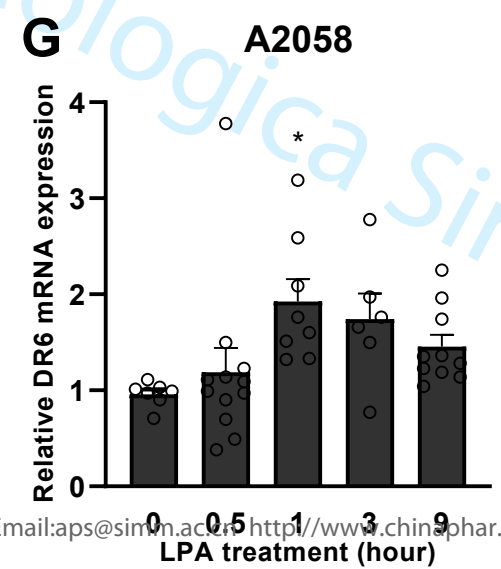

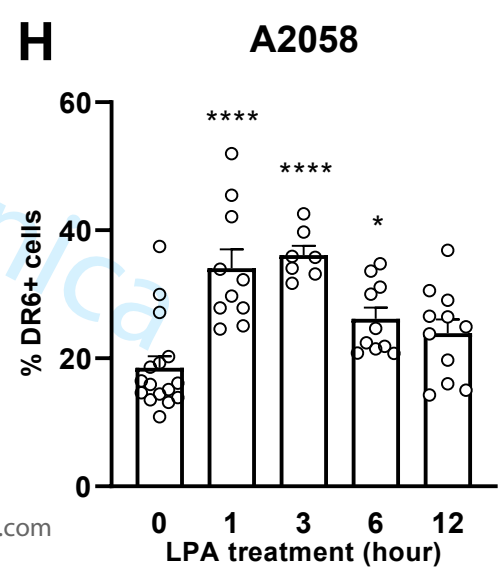

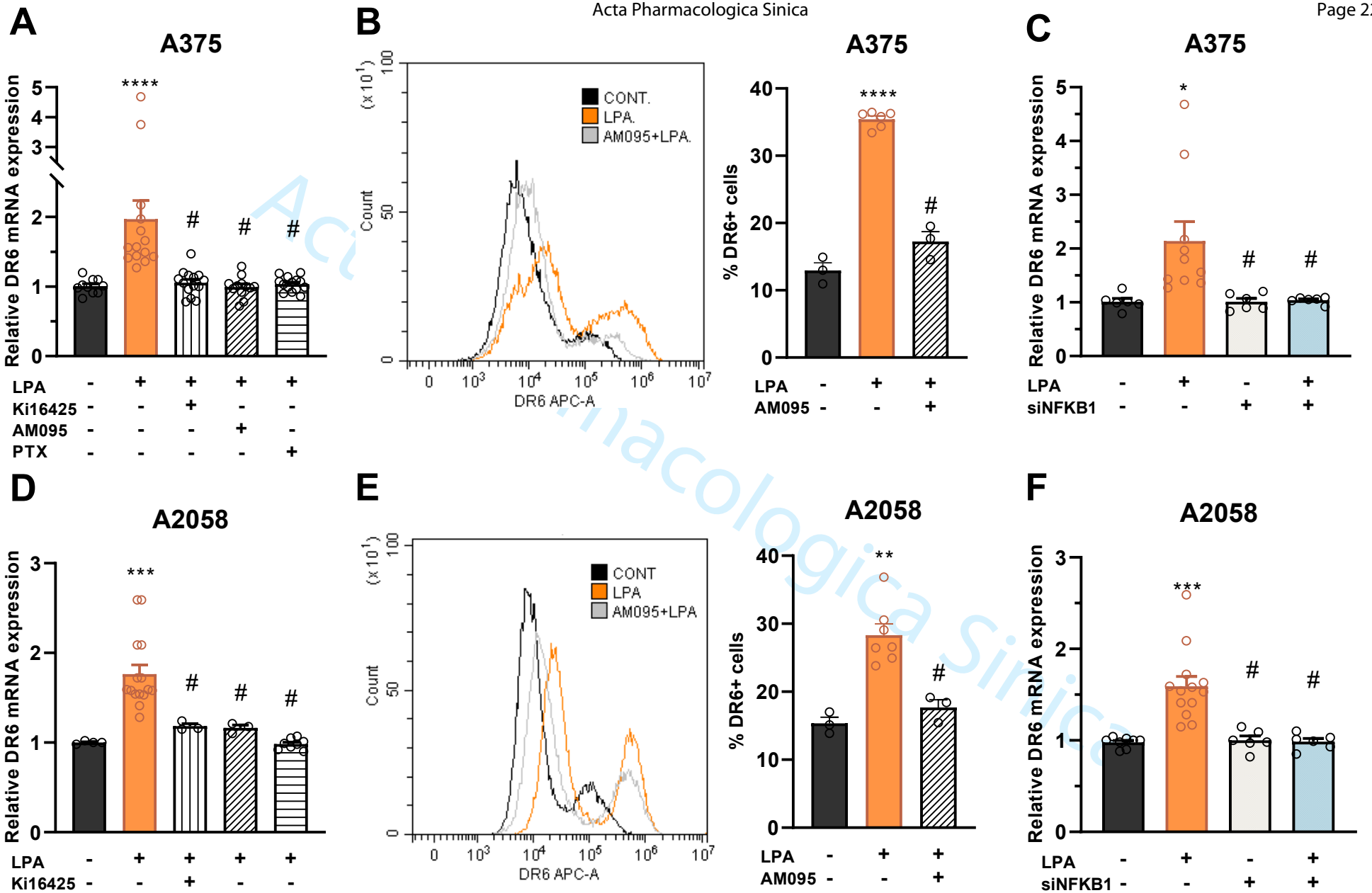

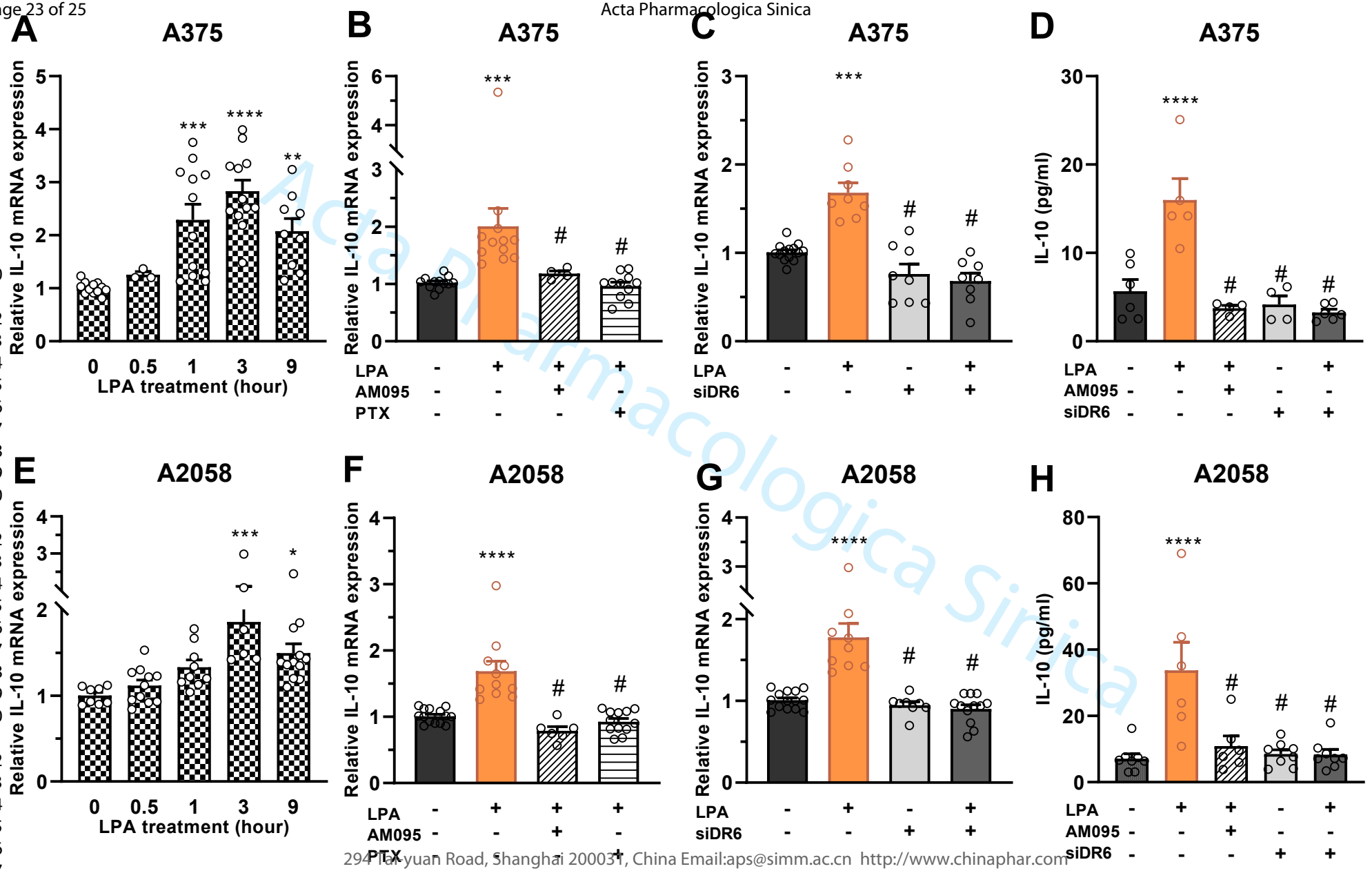

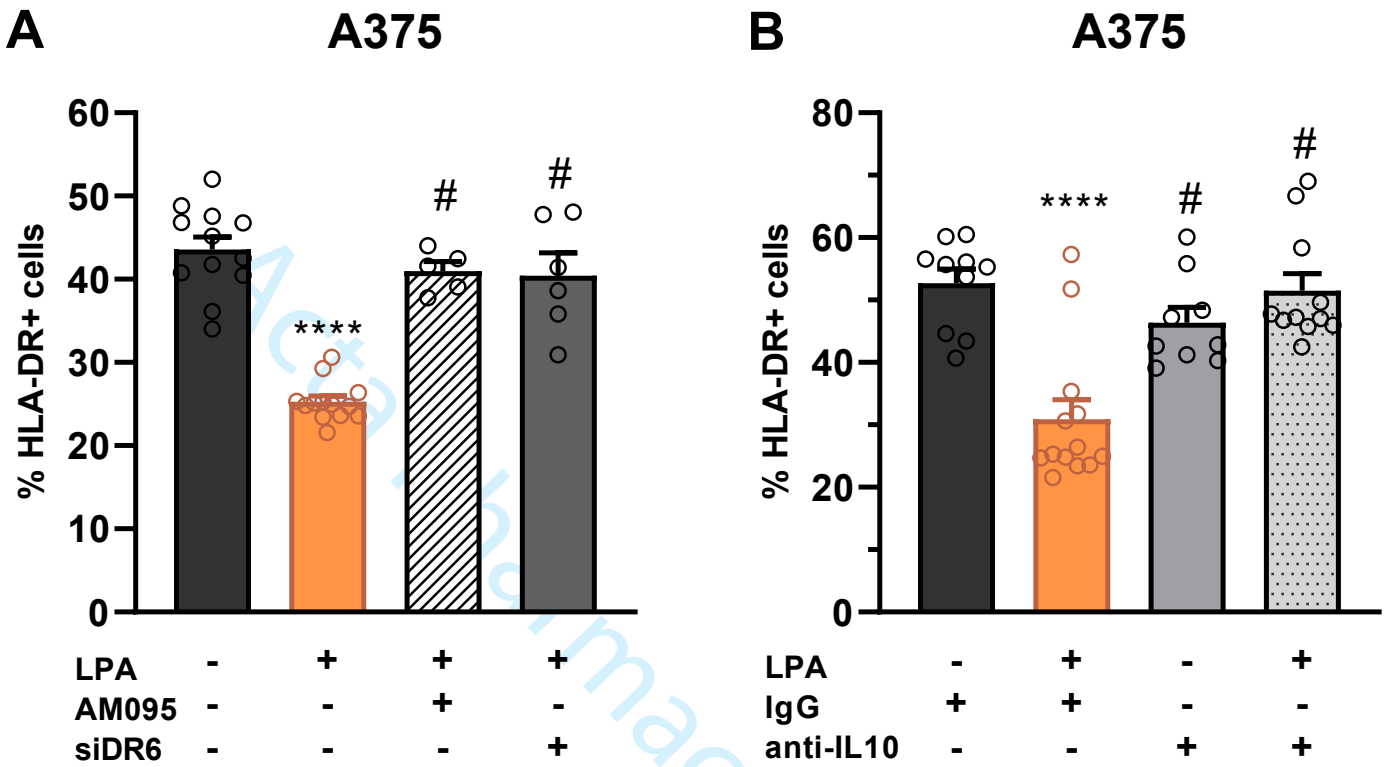

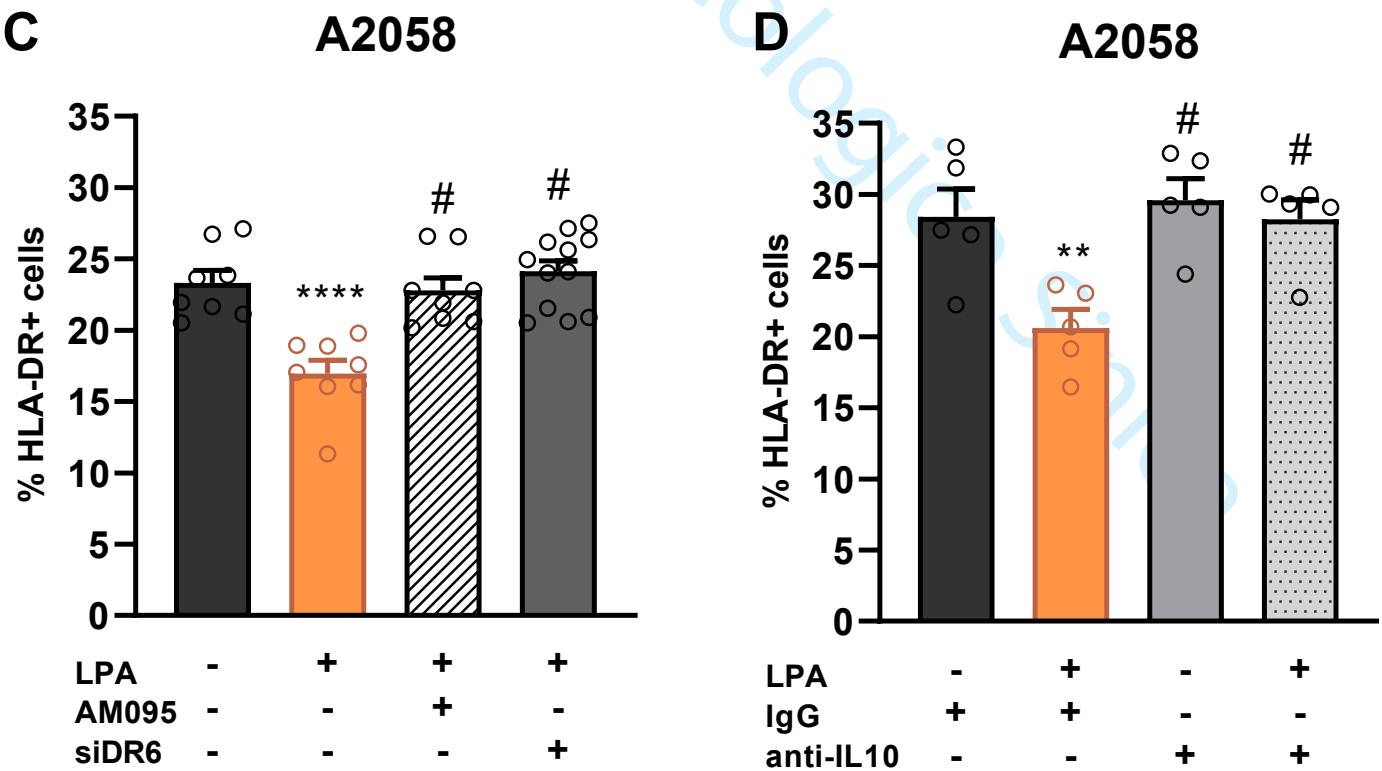

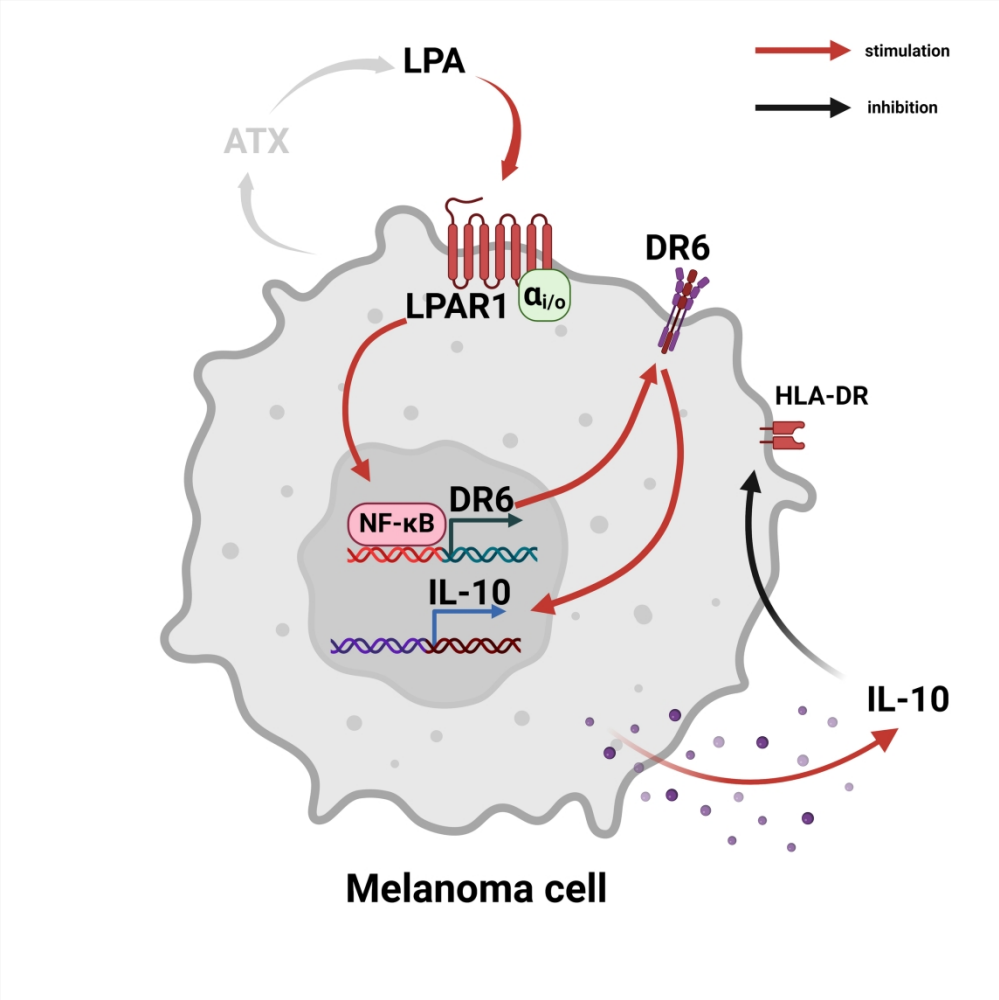

Figure 5. Signaling pathways of LPA-induced downregulation of HLA-DR in melanoma. LPA, via its Gi-coupled LPAR1 receptor, activates NF-kB-mediated DR6 expression, which in turn activates the transcription and secretion of IL-10. LPA-mediated IL-10 release leads to the downregulation of HLA-DR antigen in human melanoma cells. (Created with BioRender.com).

219x219mm (300 x 300 DPI)